

**Synthesis and characterization of 1'-(diphenylphosphino)-1-isocyanoferrocene,
an organometallic ligand combining two different soft donor moieties, and its
Group 11 metal complexes**

Karel Škoch, Ivana Císařová, Jiří Schulz, Ulrich Siemeling, and Petr Štěpnička*

Supporting Information

Contents

| | |
|--|------|
| Crystallographic data and refinement parameters (Table S1) | S-2 |
| Additional structural drawings | S-6 |
| Computed energetic parameters (Table S2) | S-15 |
| Copies of the NMR spectra | S-16 |

Table S1. Summary of crystallographic data and structure refinement parameters.^a

| Compound | 1 | 2 | 4S |
|--|--------------------------------------|--------------------------------------|---|
| Formula | C ₂₃ H ₁₈ FeNP | C ₂₂ H ₂₀ FeNP | C ₂₂ H ₁₈ FeN ₃ PS |
| <i>M</i> | 395.20 | 385.21 | 443.27 |
| Crystal system | monoclinic | triclinic | monoclinic |
| Space group | <i>P</i> 2 ₁ /c (no. 14) | <i>P</i> -1 (no. 2) | <i>P</i> 2 ₁ /n (no. 14) |
| <i>a</i> /Å | 8.9430(2) | 8.6644(4) | 13.0004(3) |
| <i>b</i> /Å | 16.7677(4) | 10.1933(4) | 8.9356(2) |
| <i>c</i> /Å | 12.9894(3) | 10.9689(5) | 34.3940(8) |
| $\alpha/^\circ$ | 90 | 103.168(1) | 90 |
| $\beta/^\circ$ | 108.1841(9) | 102.967(2) | 98.0205(8) |
| $\gamma/^\circ$ | 90 | 101.417(1) | 90 |
| <i>V</i> /Å ³ | 1850.53(7) | 887.01(7) | 3956.3(2) |
| <i>Z</i> | 4 | 2 | 8 |
| μ (Mo K α)/mm ⁻¹ | 0.907 | 0.944 | 0.962 |
| <i>F</i> (000) | 816 | 400 | 1824 |
| Diffrrns collected | 28019 | 18965 | 67506 |
| Independent diffrrns | 4258 | 4078 | 9086 |
| Observed ^b diffrrns | 3581 | 3748 | 8528 |
| <i>R</i> _{int} ^c /% | 3.44 | 2.42 | 1.94 |
| No. of parameters | 235 | 226 | 505 |
| <i>R</i> ^c obsd diffrrns/% | 2.95 | 2.39 | 4.14 |
| <i>R</i> , <i>wR</i> ^c all data/% | 3.85, 7.63 | 2.77, 5.81 | 4.41, 10.25 |
| $\Delta p/e\text{ \AA}^{-3}$ | 0.33, -0.26 | 0.27, -0.31 | 1.88, -0.95 |
| CCDC entry | 1558580 | 1558581 | 1558582 |

^a Common details: *T* = 150(2) K. ^b Diffractons with *I* > 2σ(*I*). ^c Definitions: $R_{\text{int}} = \sum |F_o^2 - F_o^2(\text{mean})| / \sum F_o^2$, where $F_o^2(\text{mean})$ is the average intensity of symmetry-equivalent diffractons. $R = \sum | |F_o| - |F_c| | / \sum |F_o|$, $wR = [\{ \sum |w| |F_o^2 - F_c^2|^2 \} / \sum |wF_o|^2]^{1/2}$.

Table S1 continued

| Compound | 4B | 5 | 6 |
|--|---|---|---|
| Formula | C ₂₂ H ₂₁ BFeN ₃ P | C ₂₃ H ₂₀ FeNOP | C ₂₃ H ₁₈ AgClFeP |
| <i>M</i> | 425.05 | 413.22 | 538.52 |
| Crystal system | monoclinic | monoclinic | triclinic |
| Space group | <i>P</i> 2 ₁ / <i>c</i> (no. 14) | <i>P</i> 2 ₁ / <i>c</i> (no. 14) | <i>P</i> -1 (no. 2) |
| <i>a</i> /Å | 9.9966(2) | 7.7210(3) | 8.3719(2) |
| <i>b</i> /Å | 15.9714(4) | 26.8385(8) | 9.6949(3) |
| <i>c</i> /Å | 12.5443(3) | 9.5519(3) | 13.6401(4) |
| $\alpha/^\circ$ | 90 | 90 | 110.216(1) |
| $\beta/^\circ$ | 92.8551(8) | 99.412(1) | 103.260(1) |
| $\gamma/^\circ$ | 90 | 90 | 95.591(1) |
| <i>V</i> /Å ³ | 2000.33(8) | 1952.7(1) | 992.10(5) |
| <i>Z</i> | 4 | 4 | 2 |
| $\mu(\text{Mo K}\alpha)/\text{mm}^{-1}$ | 0.846 | 0.866 | 1.942 |
| <i>F</i> (000) | 880 | 856 | 536 |
| Diffrrns collected | 13324 | 36002 | 10290 |
| Independent diffrrns | 4583 | 4458 | 4556 |
| Observed ^c diffrrns | 4147 | 4152 | 3960 |
| <i>R</i> _{int} ^d /% | 1.69 | 2.21 | 1.92 |
| No. of parameters | 253 | 244 | 257 |
| <i>R</i> ^d obsd diffrrns/% | 3.41 | 2.50 | 2.66 |
| <i>R</i> , <i>wR</i> ^d all data/% | 3.79, 9.96 | 2.75, 6.17 | 3.29, 6.94 |
| $\Delta\rho/\text{e } \text{\AA}^{-3}$ | 0.70, -0.59 | 0.28, -0.30 | 0.66, -0.51 |
| CCDC entry | 1558583 | 1558584 | 1558585 |

Table S1 continued

| Compound | 7 | 8·3Me₂CO | 9 |
|--|--|---|---|
| Formula | C ₅₂ H ₄₈ Ag ₂ F ₁₂ Fe ₂ N ₂ O ₂ P ₂ Sb ₂ | C ₁₀₁ H ₉₀ Ag ₂ F ₁₂ Fe ₄ N ₄ O ₃ P ₄ Sb ₂ | C ₂₃ H ₁₈ AuClFeP |
| <i>M</i> | 1593.80 | 2442.29 | 627.62 |
| Crystal system | monoclinic | monoclinic | monoclinic |
| Space group | <i>P</i> 2 ₁ /c (no. 14) | <i>C</i> 2/c (no. 15) | <i>P</i> 2 ₁ /c (no. 14) |
| <i>a</i> /Å | 8.7552(3) | 29.4021(5) | 8.4598(1) |
| <i>b</i> /Å | 14.2448(5) | 21.8753(4) | 18.9243(3) |
| <i>c</i> /Å | 22.3852(7) | 18.7554(3) | 12.8116(2) |
| $\alpha/^\circ$ | 90 | 90 | 90 |
| $\beta/^\circ$ | 98.237(1) | 127.1702(5) | 94.3304(6) |
| $\gamma/^\circ$ | 90 | 90 | 90 |
| <i>V</i> /Å ³ | 2763.0(2) | 9612.4(3) | 2045.23(5) |
| <i>Z</i> | 2 | 4 | 4 |
| μ (Mo K α)/mm ⁻¹ | 2.310 | 1.680 | 8.092 |
| <i>F</i> (000) | 1552 | 4864 | 1200 |
| Diffrrns collected | 48377 | 38105 | 16559 |
| Independent diffrrns | 6354 | 11055 | 4692 |
| Observed ^c diffrrns | 5398 | 9073 | 4097 |
| <i>R</i> _{int} ^d /% | 3.59 | 2.41 | 2.80 |
| No. of parameters | 345 | 600 | 257 |
| <i>R</i> ^d obsd diffrrns/% | 3.77 | 3.07 | 1.93 |
| <i>R</i> , <i>wR</i> ^d all data/% | 4.59, 9.82 | 4.14, 7.83 | 2.58, 3.99 |
| $\Delta\rho/e\text{ \AA}^{-3}$ | 2.24, -2.43 | 1.79, -1.70 | 0.78, -0.41 |
| CCDC entry | 1558586 | 1558587 | 1558588 |

Table S1 continued

| Compound | 10 | 11a·2Me₂CO |
|--|--|--|
| Formula | C ₂₃ H ₁₈ Au ₂ Cl ₂ FeNP | C ₅₂ H ₄₈ Au ₂ F ₁₂ Fe ₂ N ₂ O ₂ P ₂ Sb ₂ |
| <i>M</i> | 860.04 | 1772.00 |
| Crystal system | triclinic | monoclinic |
| Space group | <i>P</i> -1 (no. 2) | <i>P</i> 2 ₁ /c (no. 14) |
| <i>a</i> /Å | 7.7090(2) | 8.8480(3) |
| <i>b</i> /Å | 10.0529(3) | 14.2781(9) |
| <i>c</i> /Å | 15.6084(4) | 22.257(1) |
| $\alpha/^\circ$ | 90.179(1) | 90 |
| $\beta/^\circ$ | 100.158(1) | 98.795(2) |
| $\gamma/^\circ$ | 107.216(1) | 90 |
| <i>V</i> /Å ³ | 1135.34(5) | 2778.7(2) |
| <i>Z</i> | 2 | 2 |
| μ (Mo K α)/mm ⁻¹ | 2.516 | 6.866 |
| <i>F</i> (000) | 792 | 1680 |
| Diffrns collected | 15177 | 21495 |
| Independent diffrns | 5212 | 6333 |
| Observed ^c diffrns | 4531 | 5599 |
| <i>R</i> _{int} ^d /% | 2.47 | 2.82 |
| No. of parameters | 271 | 345 |
| <i>R</i> ^d obsd diffrns/% | 2.14 | 2.58 |
| <i>R</i> , <i>wR</i> ^d all data/% | 2.79, 4.48 | 3.20, 5.39 |
| $\Delta\rho/e\text{ \AA}^{-3}$ | 1.03, -0.93 | 1.36, -1.34 |
| CCDC entry | 1558589 | 1558590 |

Additional structural diagrams

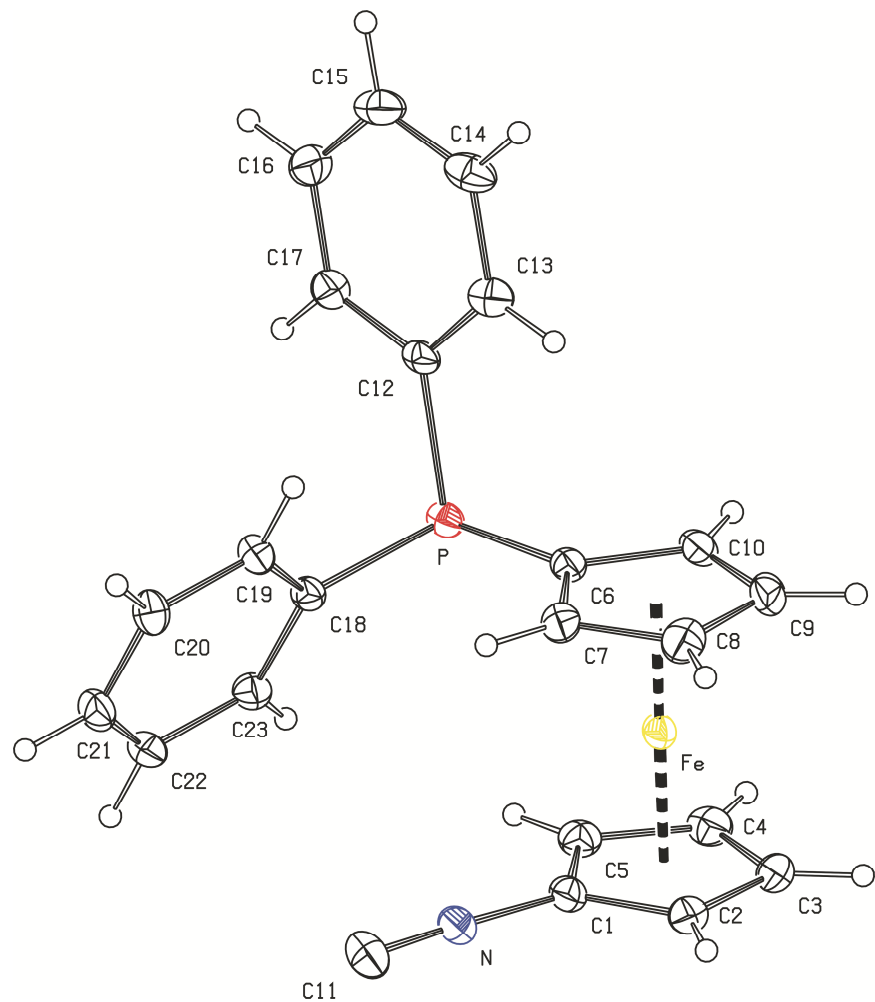


Figure S1. PLATON plot of the molecular structure of **1** showing displacement ellipsoids at the 30% probability level.

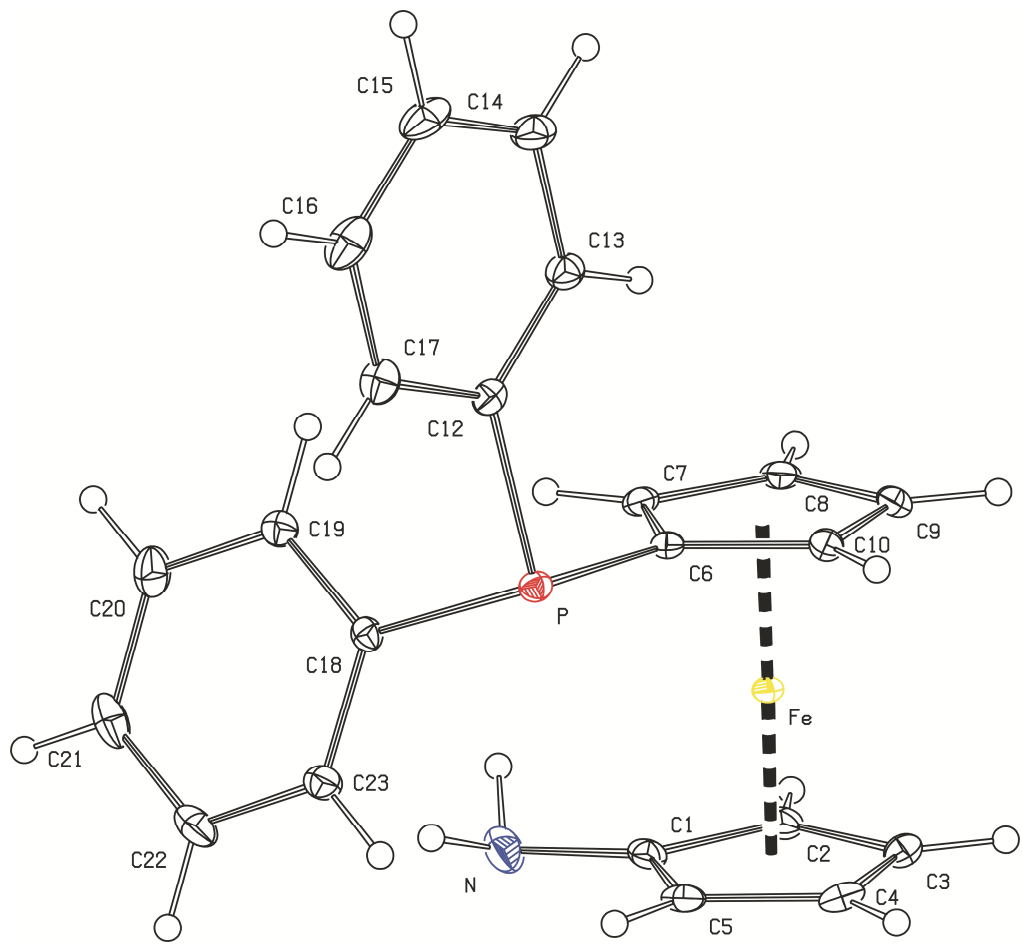


Figure S2. PLATON plot of the molecular structure of **2** showing displacement ellipsoids at the 30% probability level.

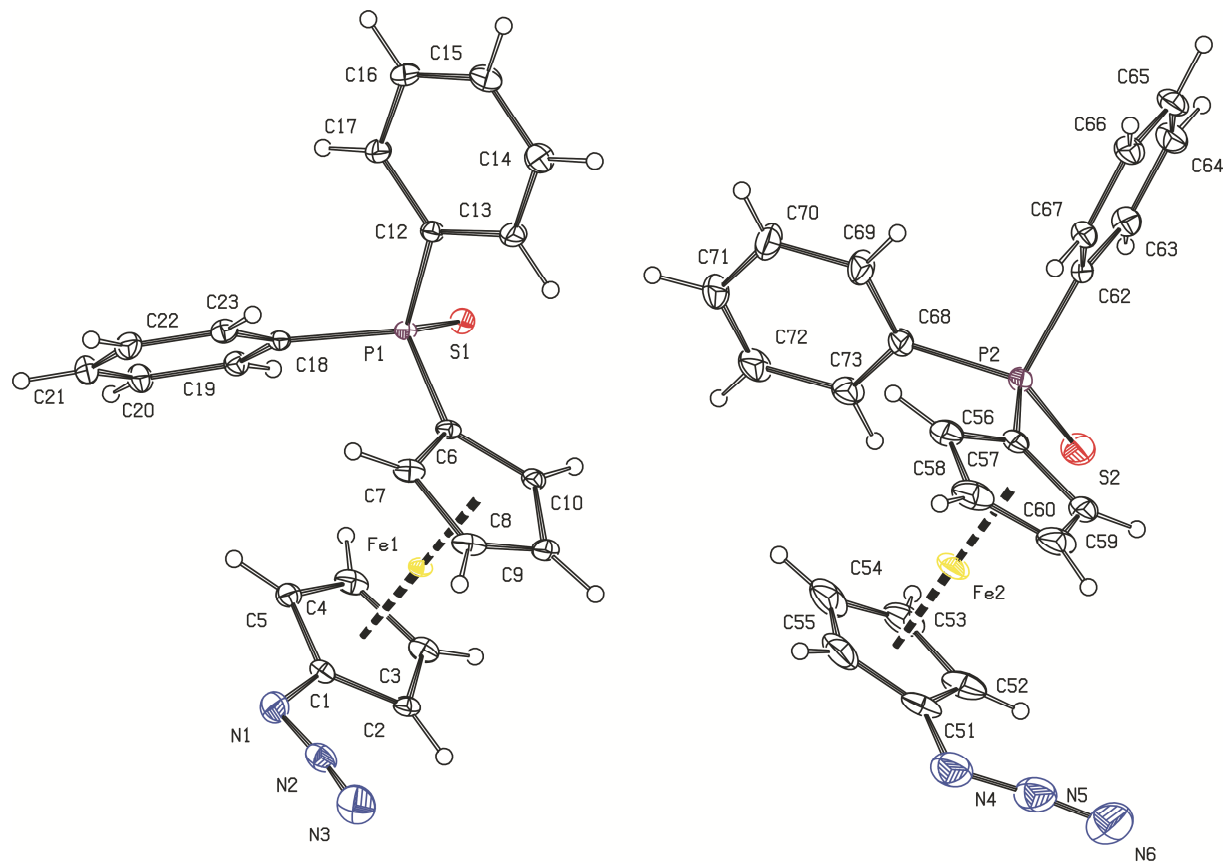


Figure S3. PLATON plot of the two crystallographically independent molecules of **4S** showing displacement ellipsoids at the 30% probability level.

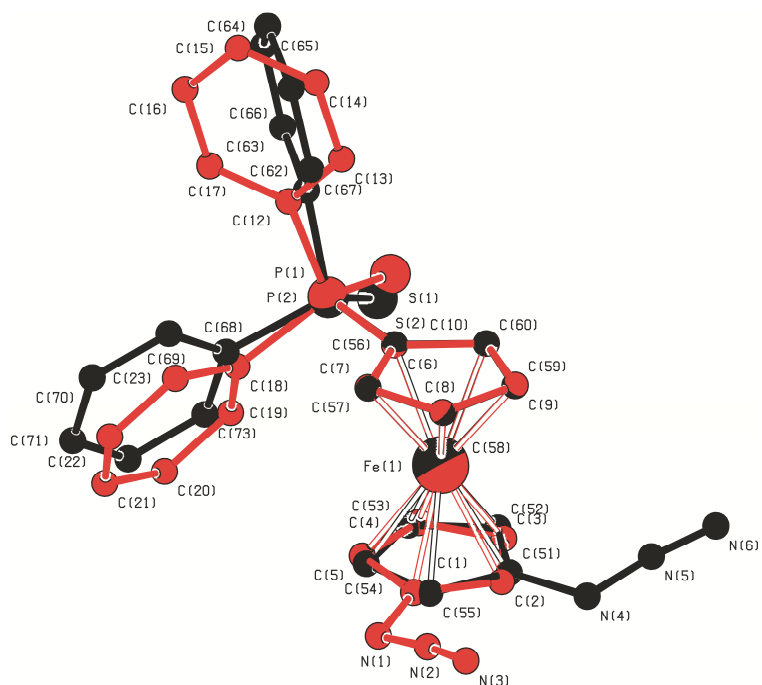


Figure S4. Overlap of the two crystallographically independent molecules of **4S**.

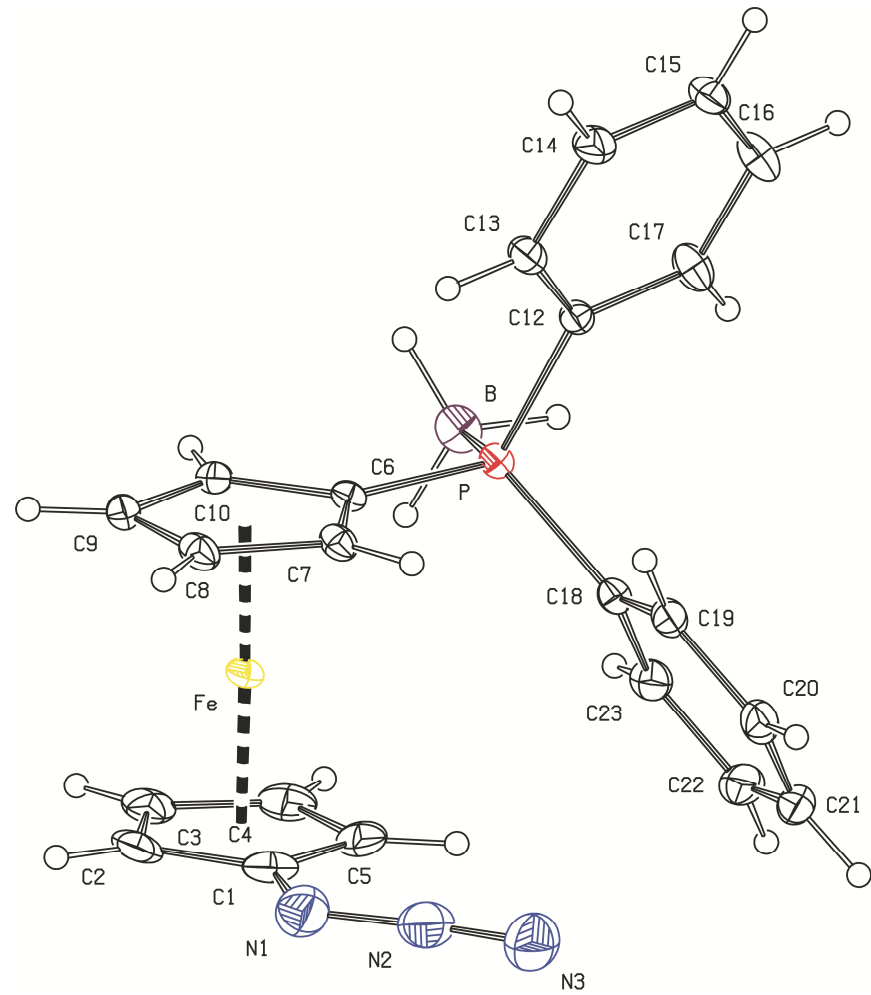


Figure S5. PLATON plot of the molecular structure of **4B** showing displacement ellipsoids at the 30% probability level.

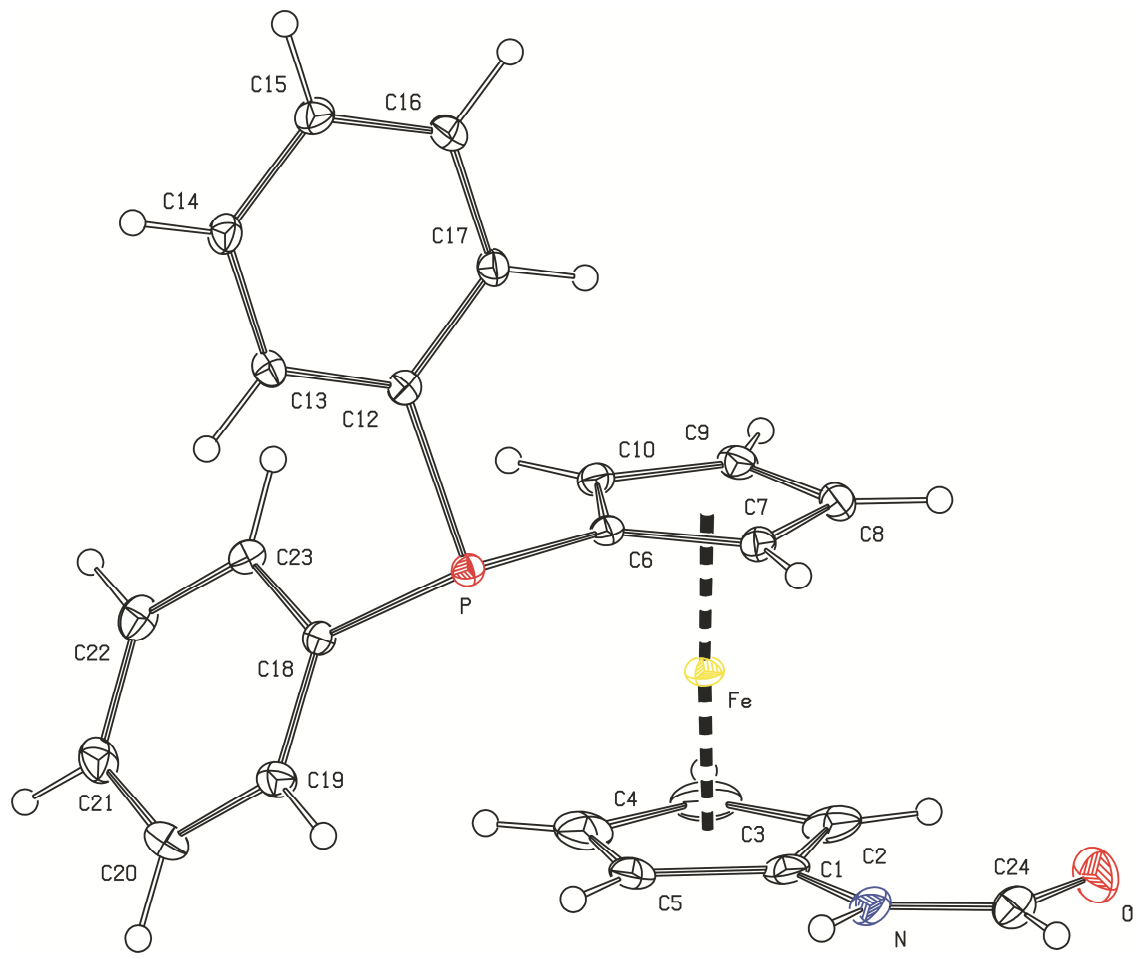


Figure S6. PLATON plot of the molecular structure of **5** showing displacement ellipsoids at the 30% probability level.

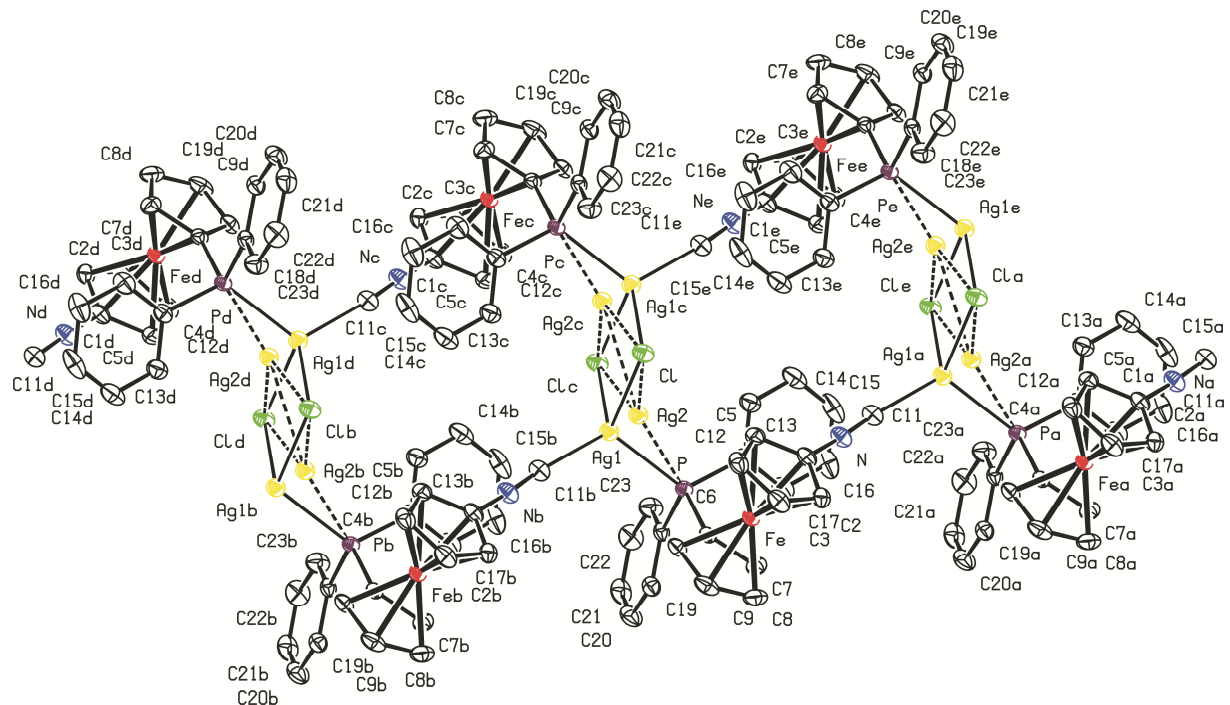


Figure S7. PLATON plot of the infinite assembly in the structure of **6** with displacement ellipsoids at the 30% probability level. Hydrogen atoms are omitted for clarity.

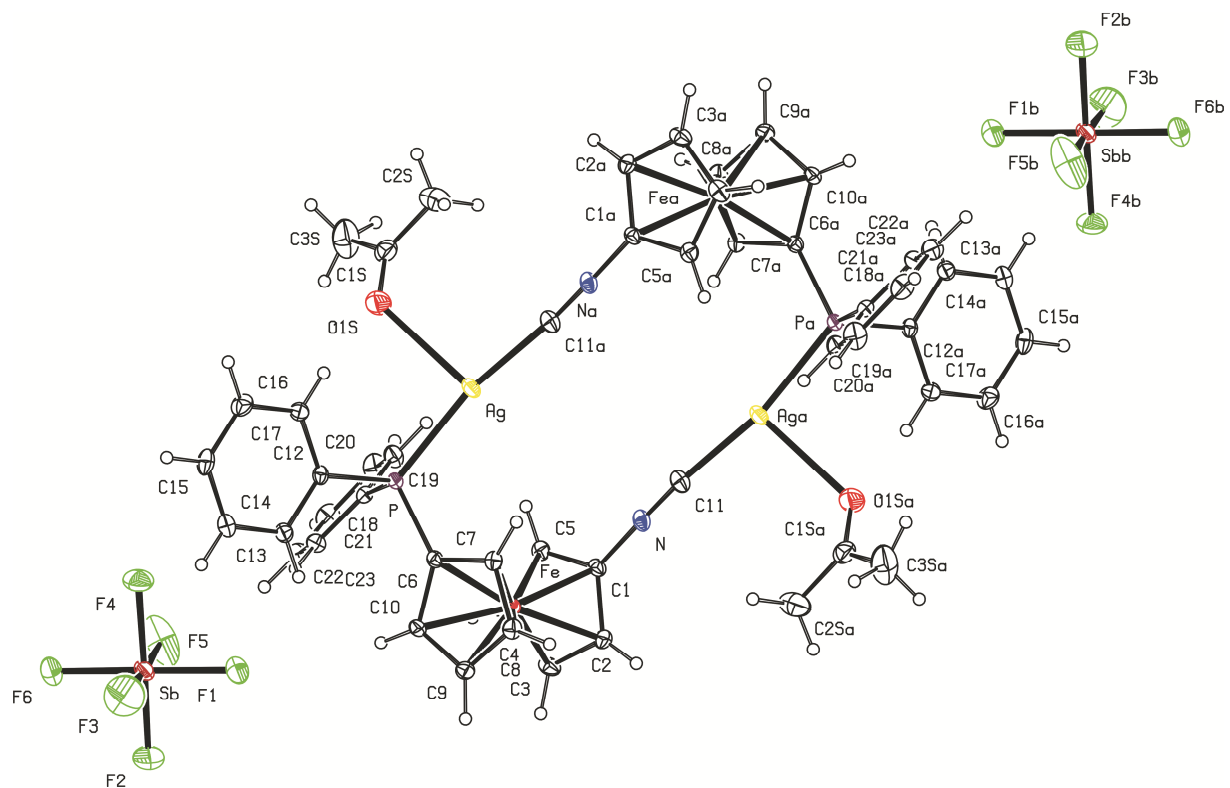


Figure S8. PLATON plot of the molecular structure of **7** showing displacement ellipsoids at the 30% probability level.

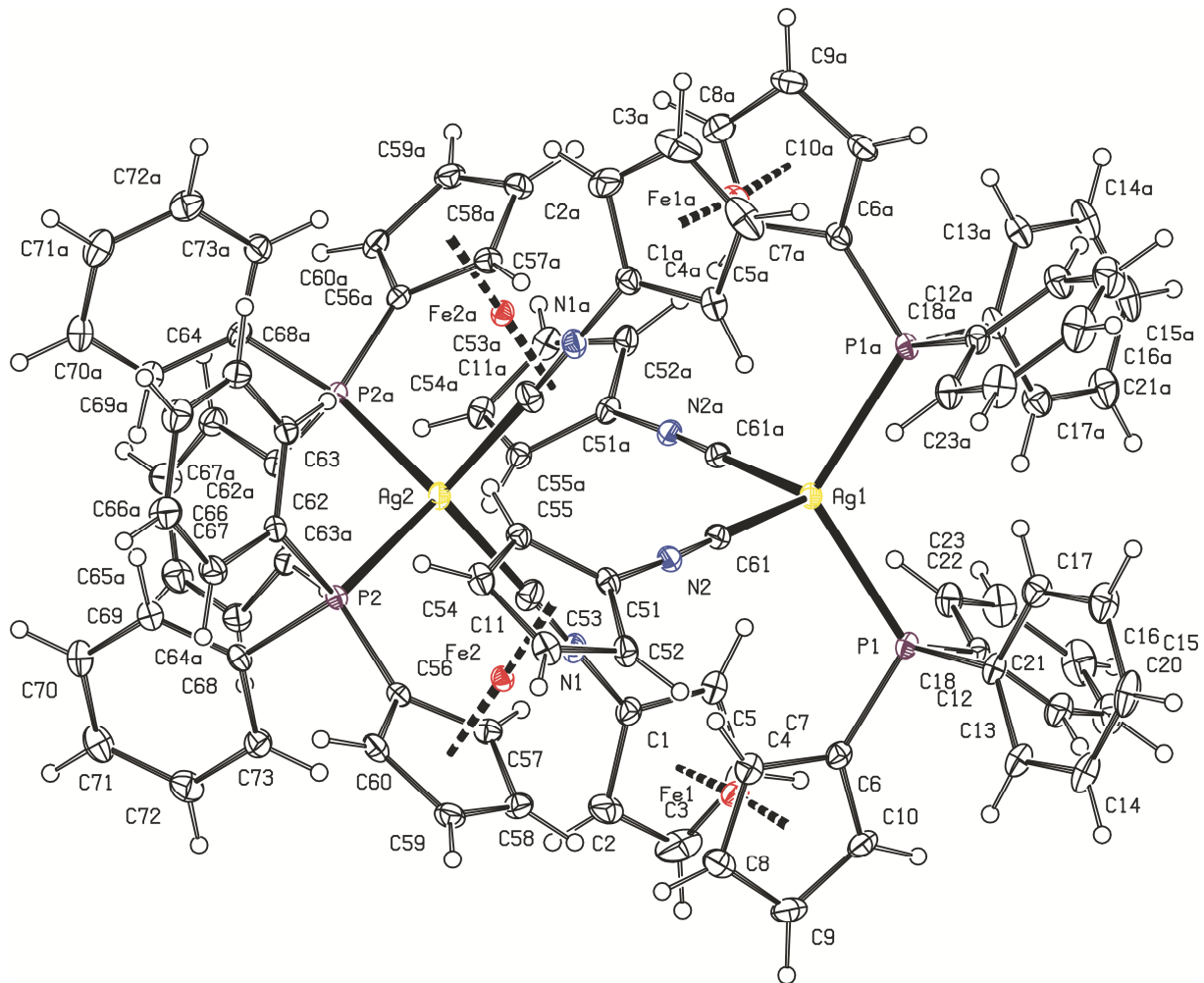


Figure S9. PLATON plot of the complex cation in the structure of **8**·3Me₂CO showing displacement ellipsoids at the 30% probability level.

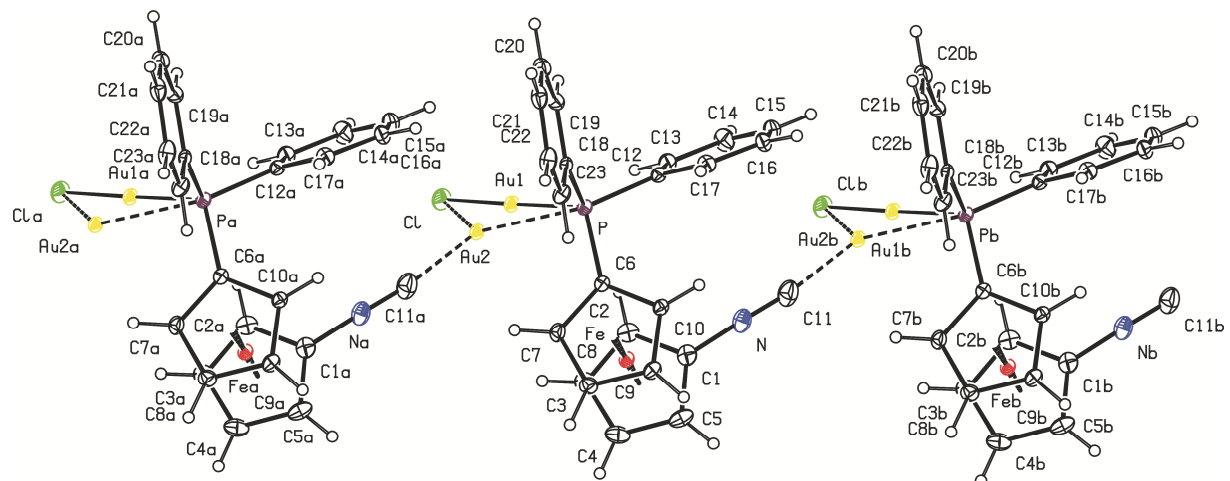


Figure S10. PLATON plot of the structure of **9** showing displacement ellipsoids at the 30% probability level.

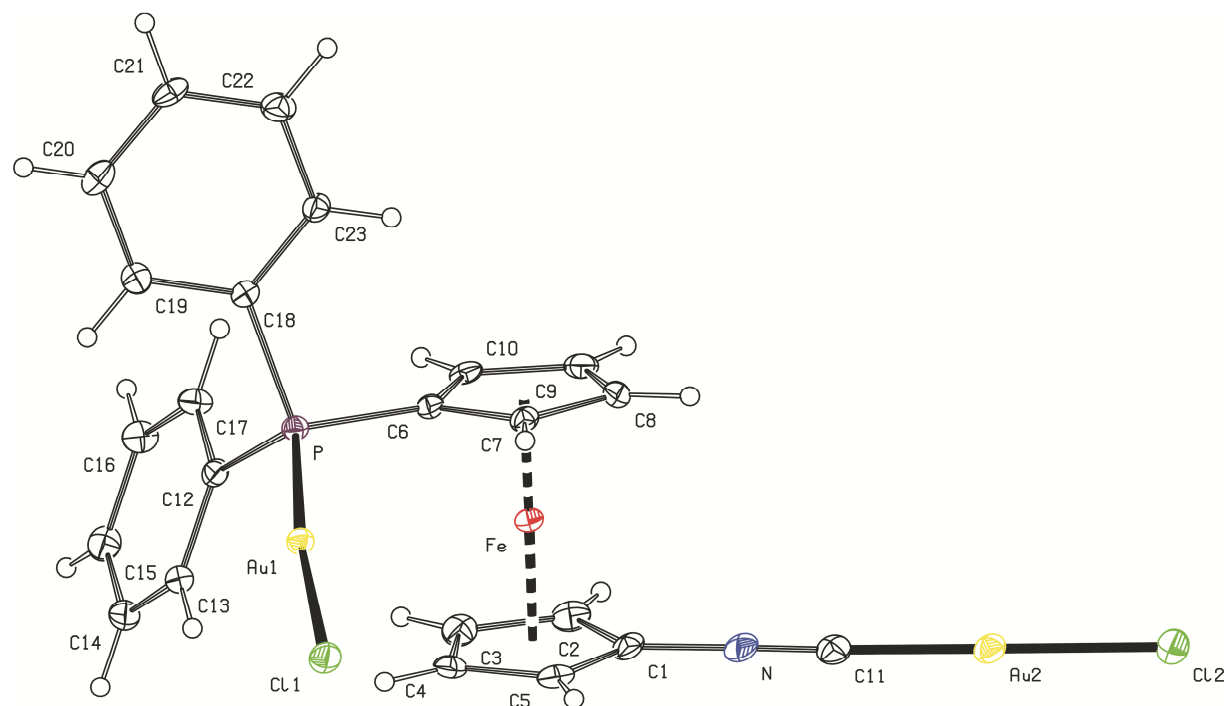


Figure S11. PLATON plot of the molecular structure of **10** showing displacement ellipsoids at the 30% probability level.

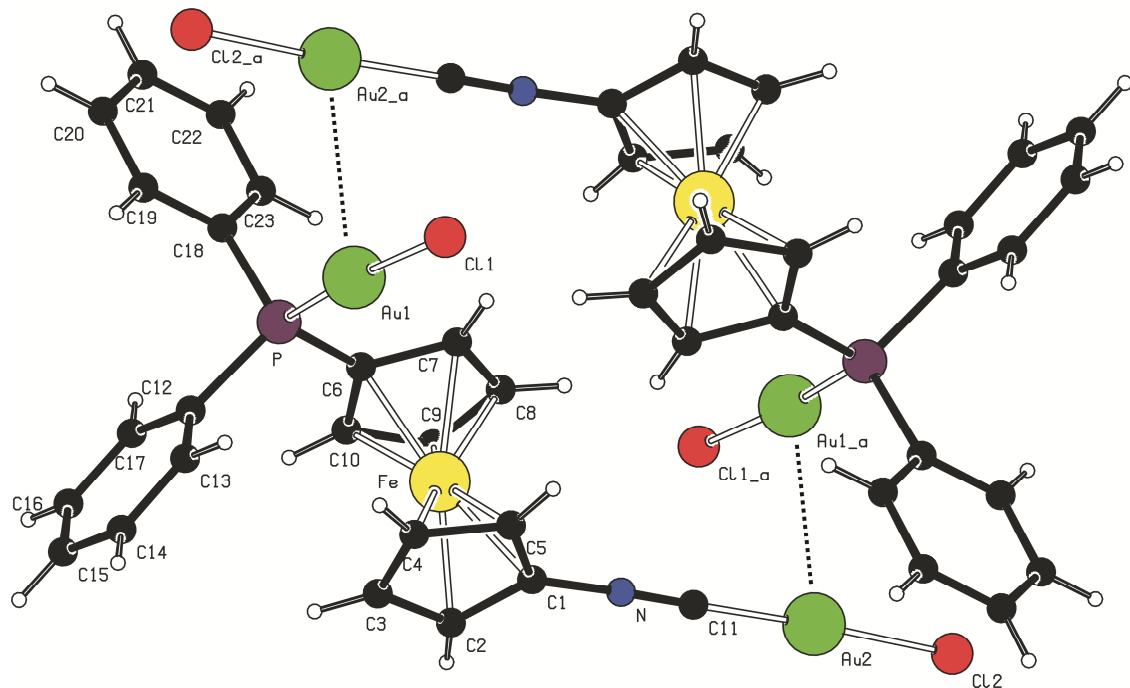


Figure S12. Possible Au...Au contacts in the structure of **10**.

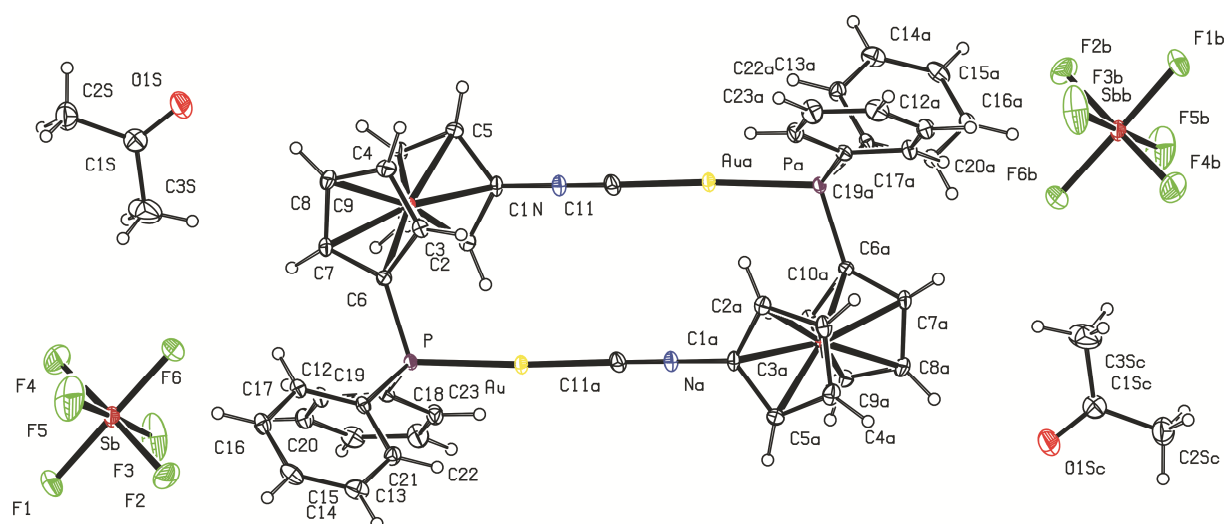


Figure S13. PLATON plot of the molecular structure of **11a**·2Me₂CO showing displacement ellipsoids at the 30% probability level.

Table S2. Summary of computed energetic parameters^a

| Compound | <i>E</i> (Hartree) | ZPE (Hartree) | <i>G</i> (kcal mol ⁻¹) |
|--|--------------------|---------------|------------------------------------|
| [Au ₂ (m(P,N)- D) ₂] ²⁺ | -3083.470112 | 0.693103 | -3082.867457 |
| [Au D] ¹⁺ | -1541.701959 | 0.345266 | -1541.412095 |
| [Au ₂ (m(P,C)- 11) ₂] ²⁺ | -3083.435496 | 0.69292 | -3082.830992 |
| [Au(11)] ¹⁺ | -1541.675001 | 0.345159 | -1541.384068 |

^a Gaussian energetic parameters calculated at the PBE0/ccPVDZ:sdd(Fe,Au) level of theory.

Copies of the NMR spectra (newly prepared compounds only)

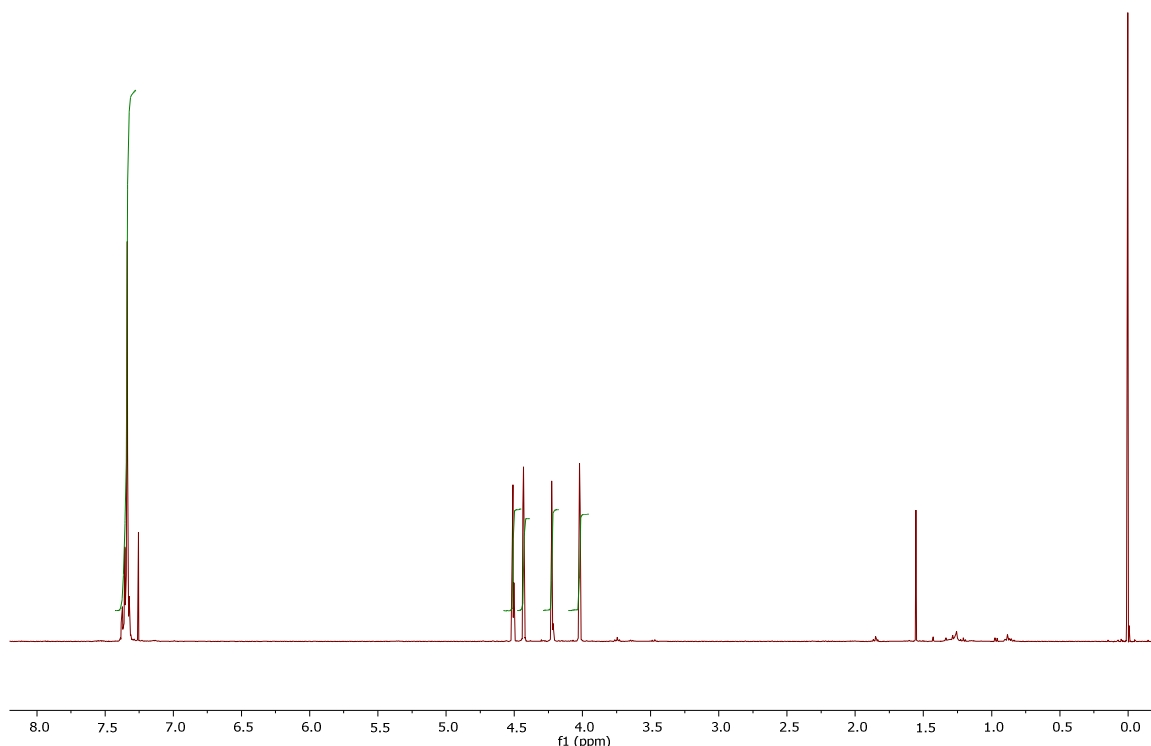


Figure S14. ^1H NMR spectrum of **1** (CDCl_3).

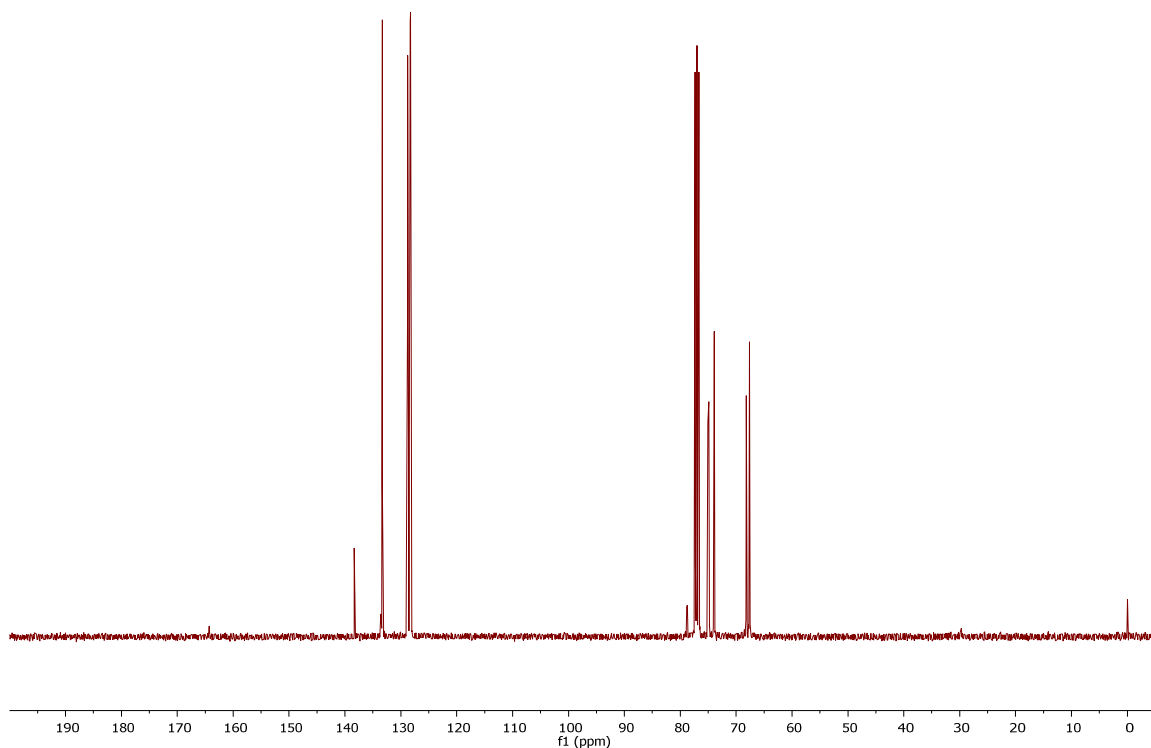


Figure S15. $^{13}\text{C}\{^1\text{H}\}$ NMR spectrum of **1** (CDCl_3).

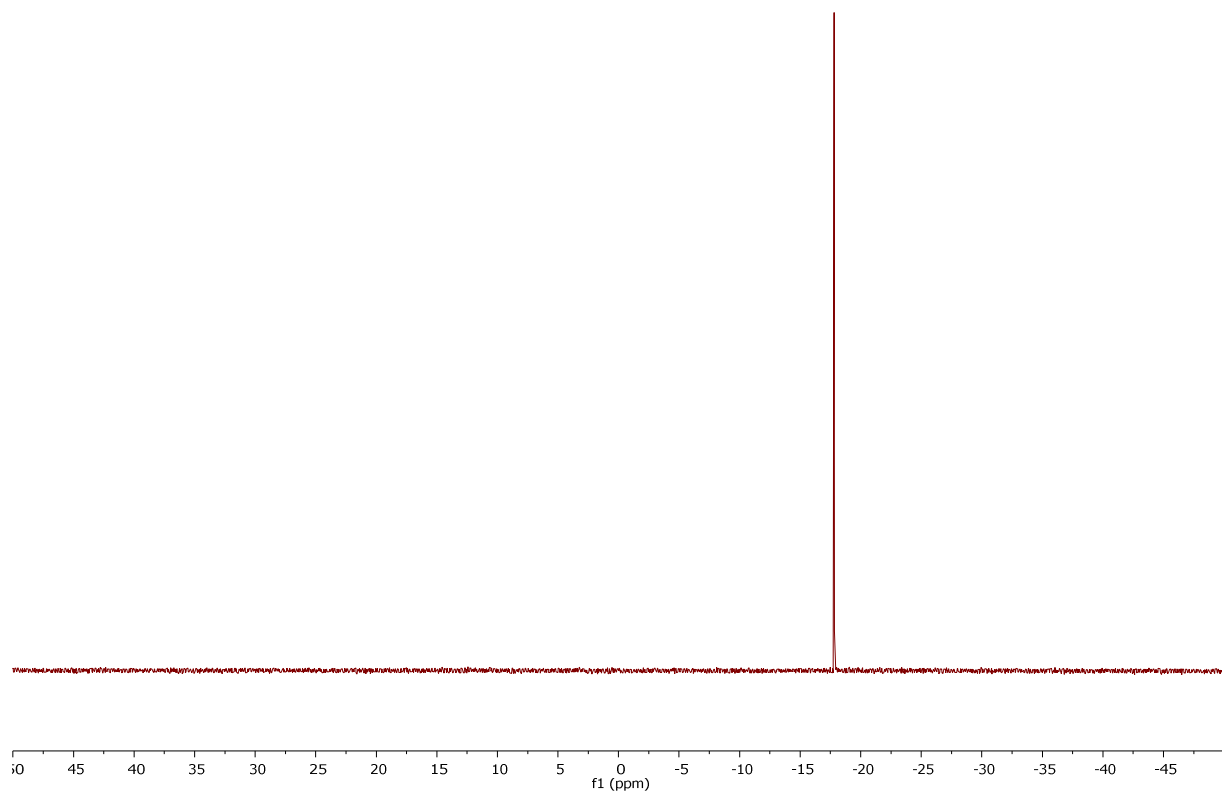


Figure S16. $^{31}\text{P}\{\text{H}\}$ NMR spectrum of **1** (CDCl_3).

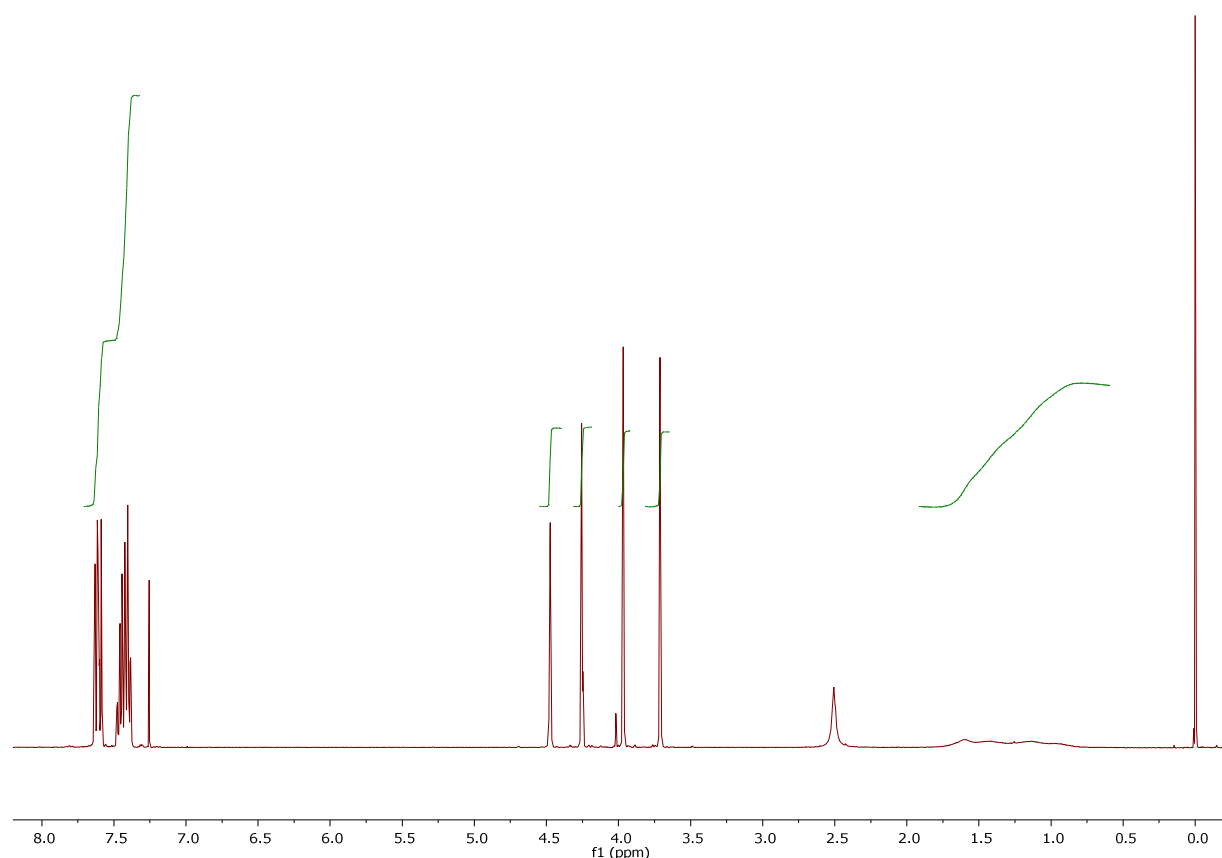


Figure S17. ^1H NMR spectrum of **2B** (CDCl_3).

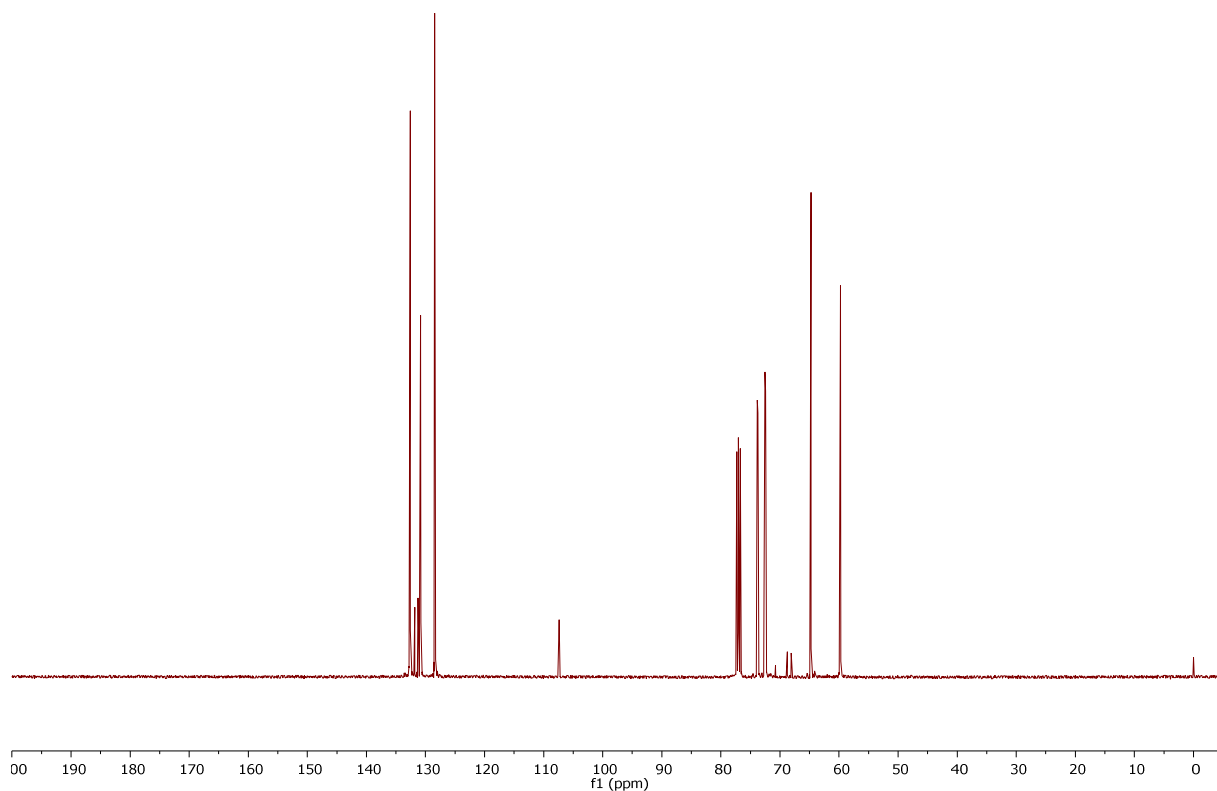


Figure S18. $^{13}\text{C}\{\text{H}\}$ NMR spectrum of **2B** (CDCl_3).

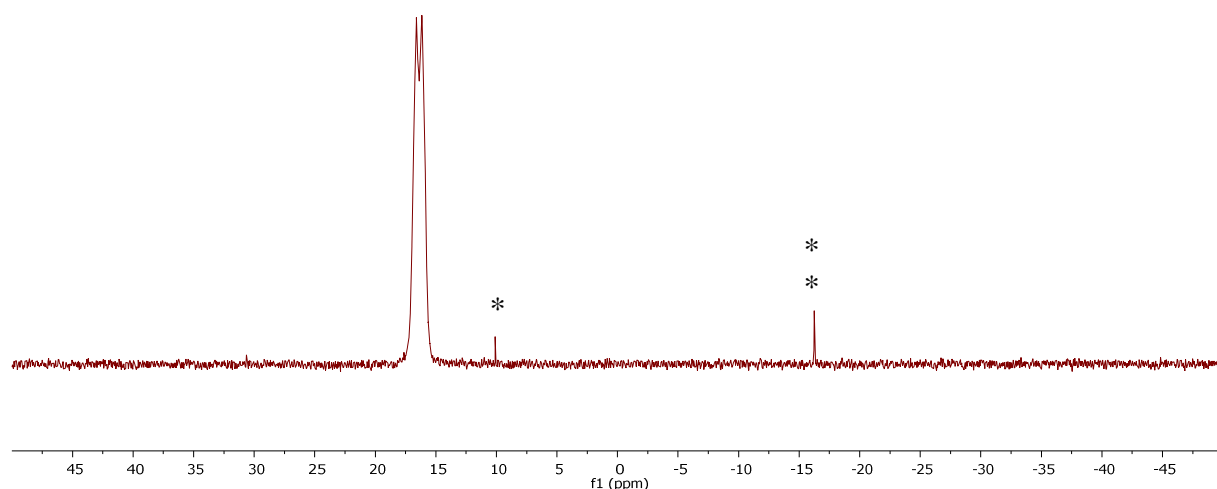


Figure S19. $^{31}\text{P}\{\text{H}\}$ NMR spectrum of **2B** (CDCl_3 ; * = system peak; ** = **2**).

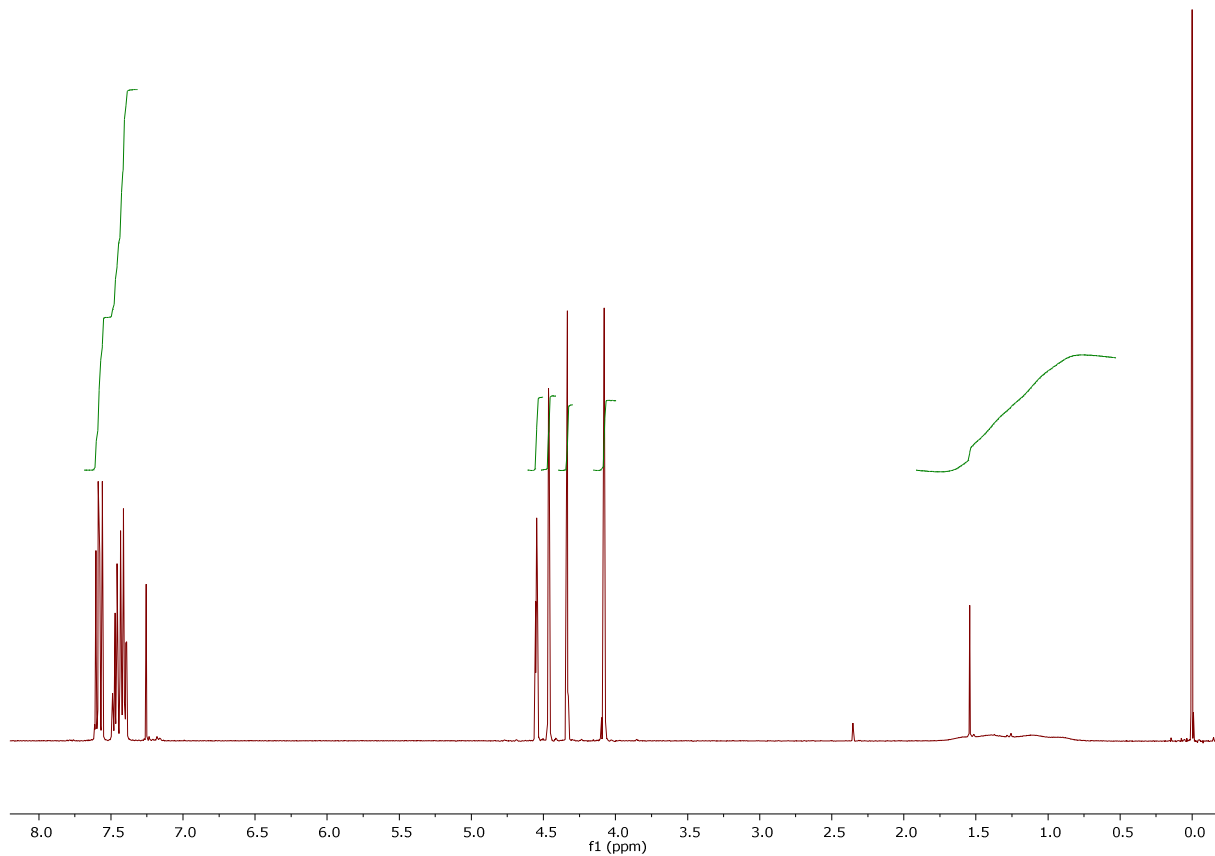


Figure S20. ^1H NMR spectrum of **3B** (CDCl_3).

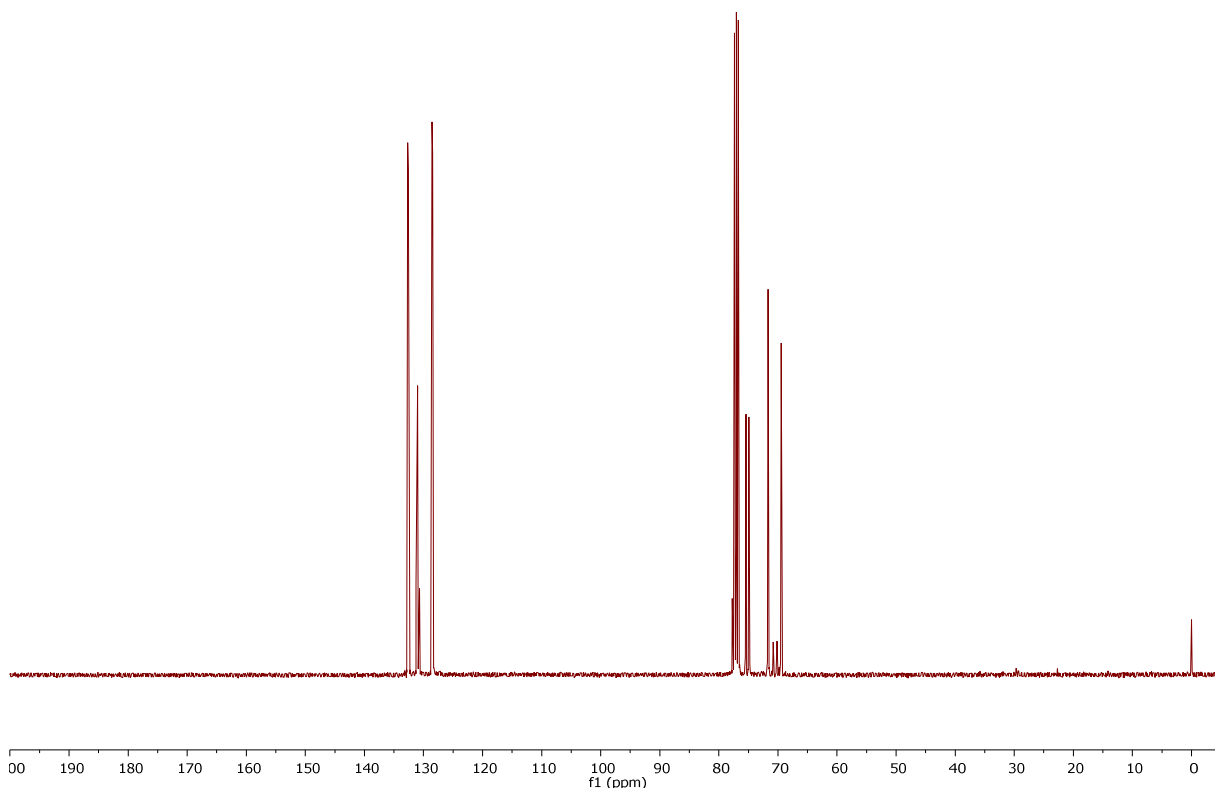


Figure S21. $^{13}\text{C}\{\text{H}\}$ NMR spectrum of **3B** (CDCl_3).

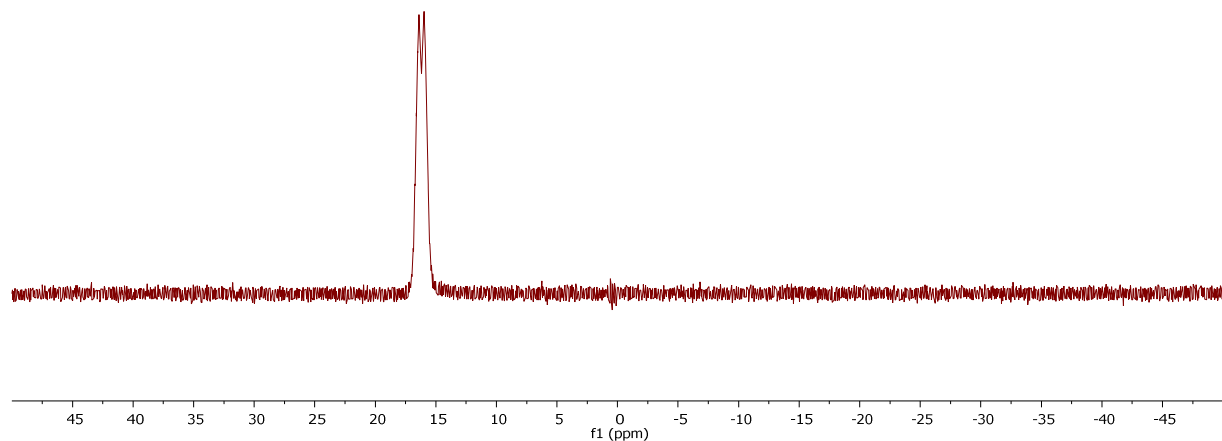


Figure S22. $^{31}\text{P}\{\text{H}\}$ NMR spectrum of **3B** (CDCl_3).

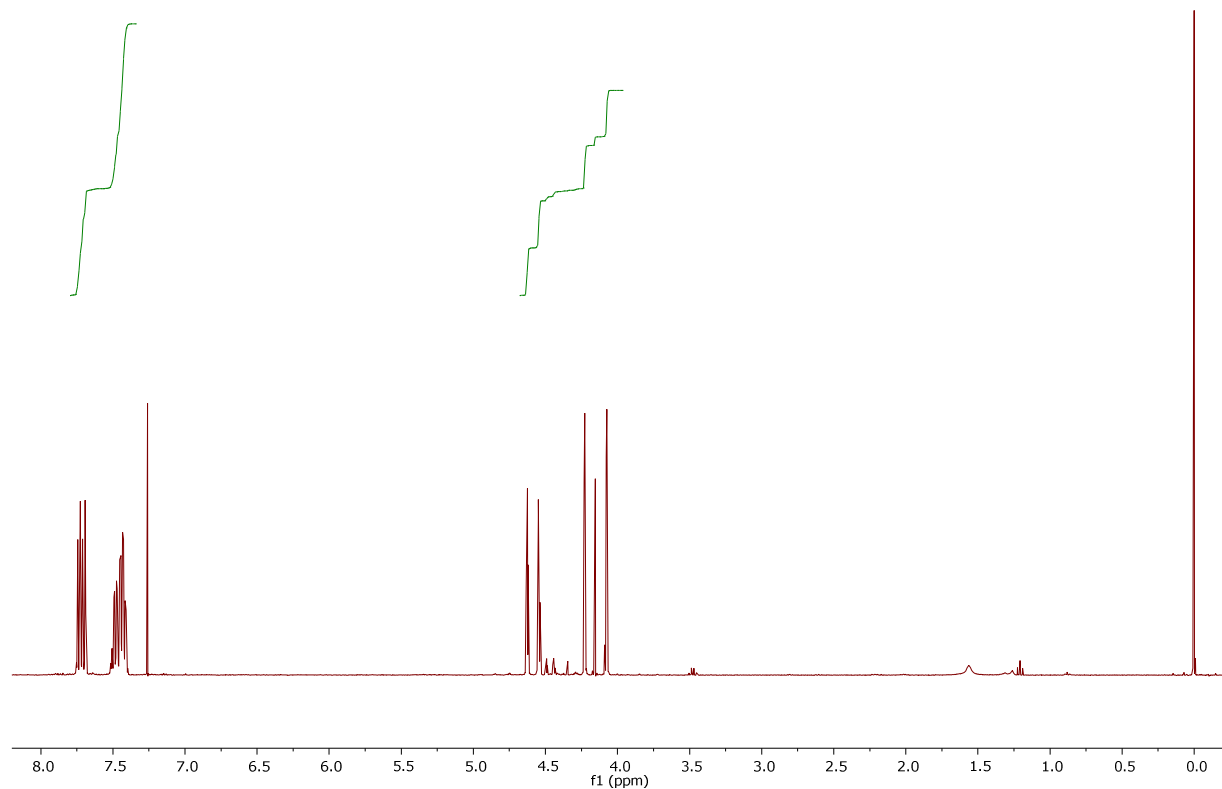


Figure S23. ^1H NMR spectrum of **4S** (CDCl_3).

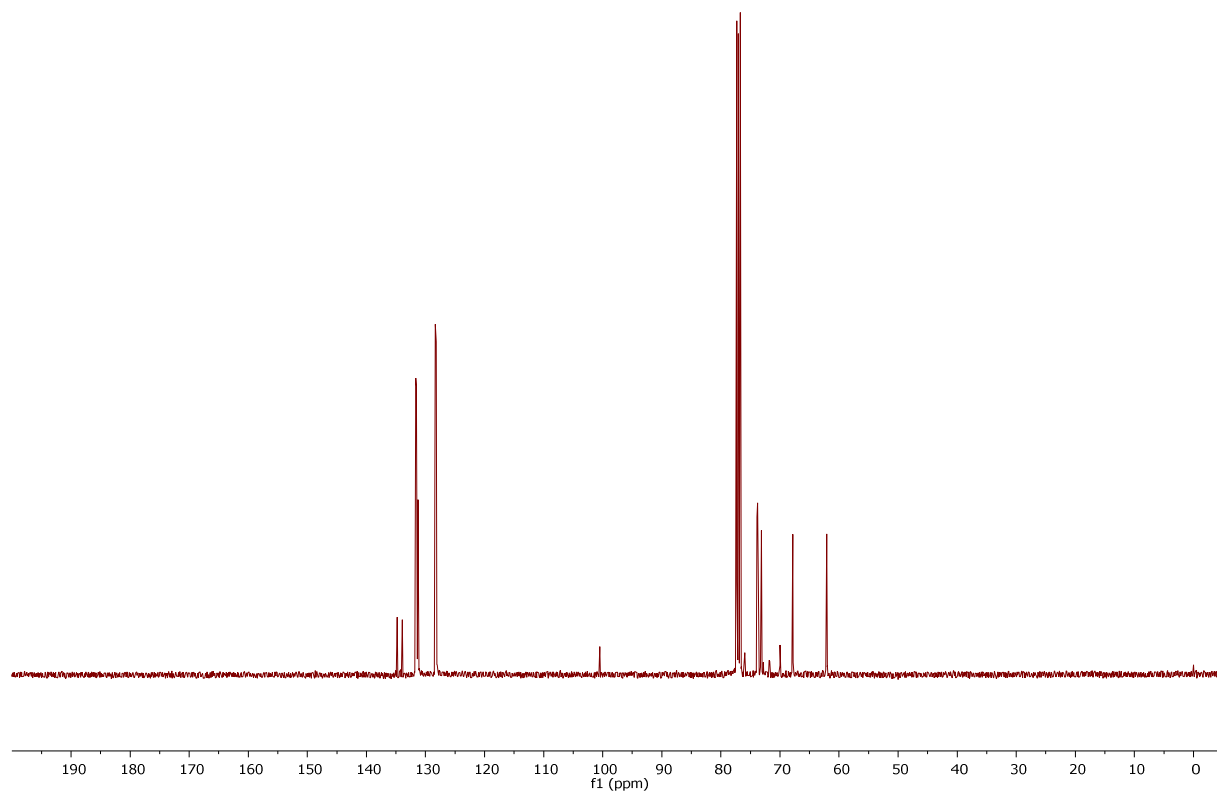


Figure S24. $^{13}\text{C}\{\text{H}\}$ NMR spectrum of **4S** (CDCl_3).

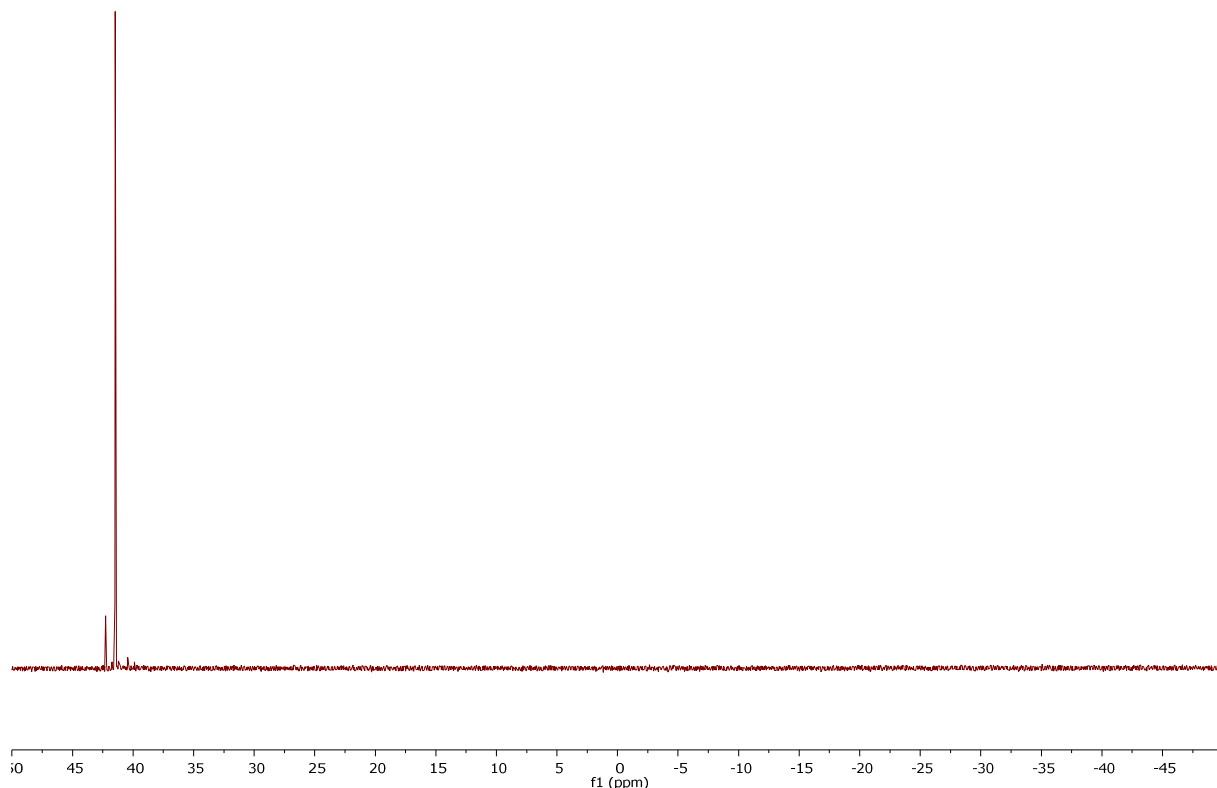


Figure S25. $^{31}\text{P}\{\text{H}\}$ NMR spectrum of **4S** (CDCl_3).

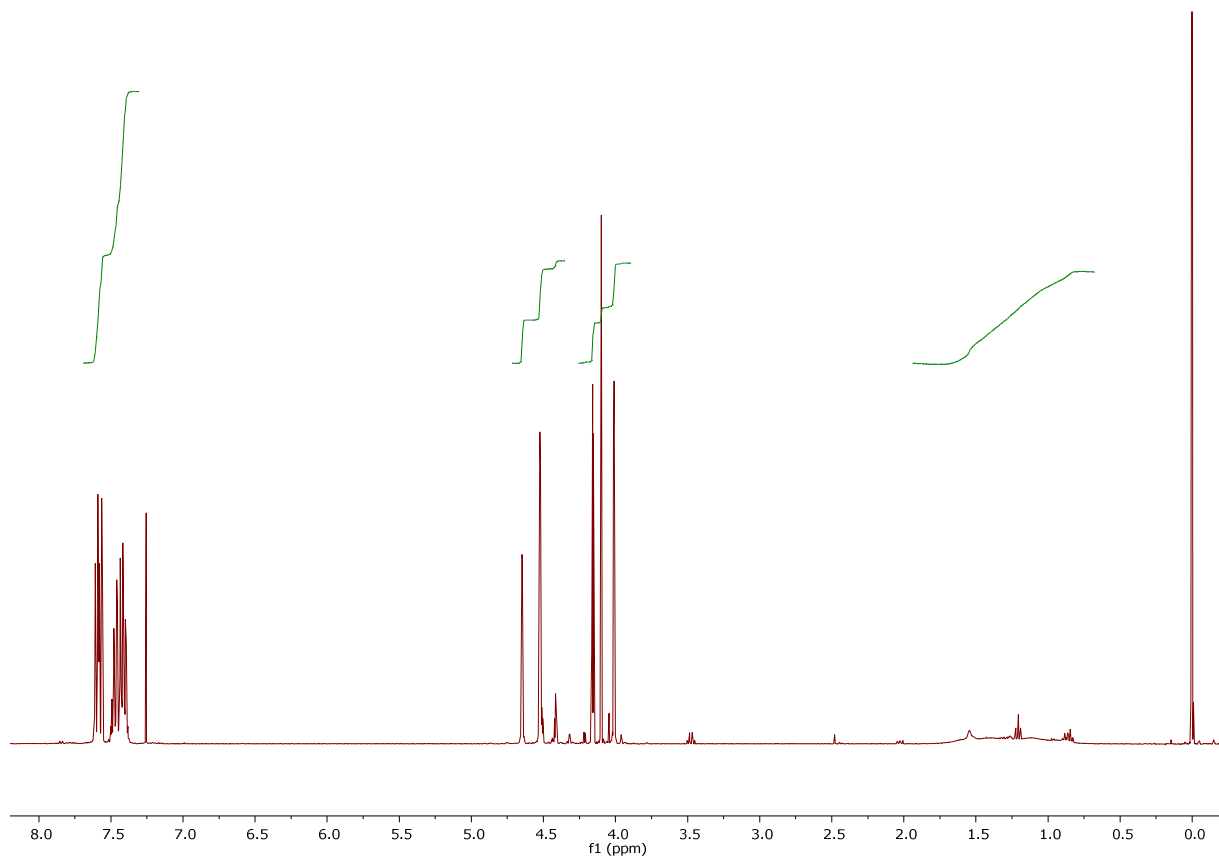


Figure S26. ^1H NMR spectrum of **4B** (CDCl_3).

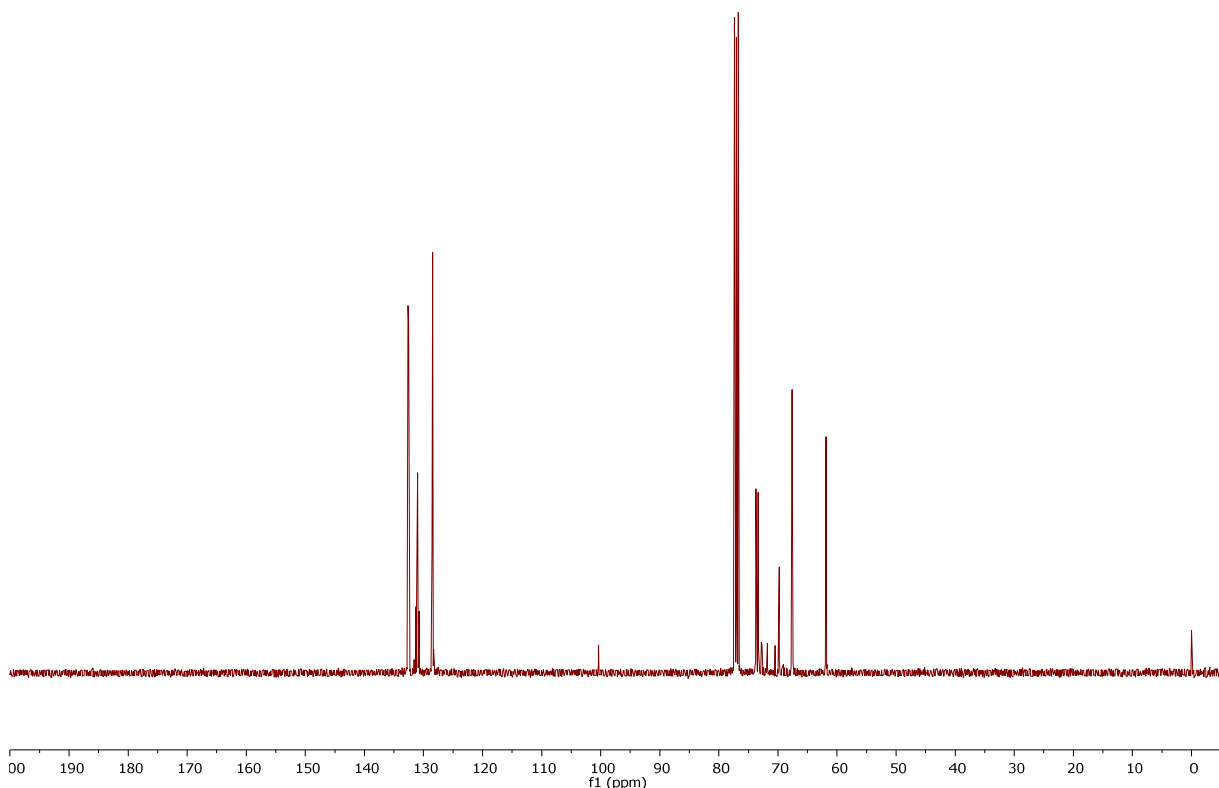


Figure S27. $^{13}\text{C}\{\text{H}\}$ NMR spectrum of **4B** (CDCl_3).

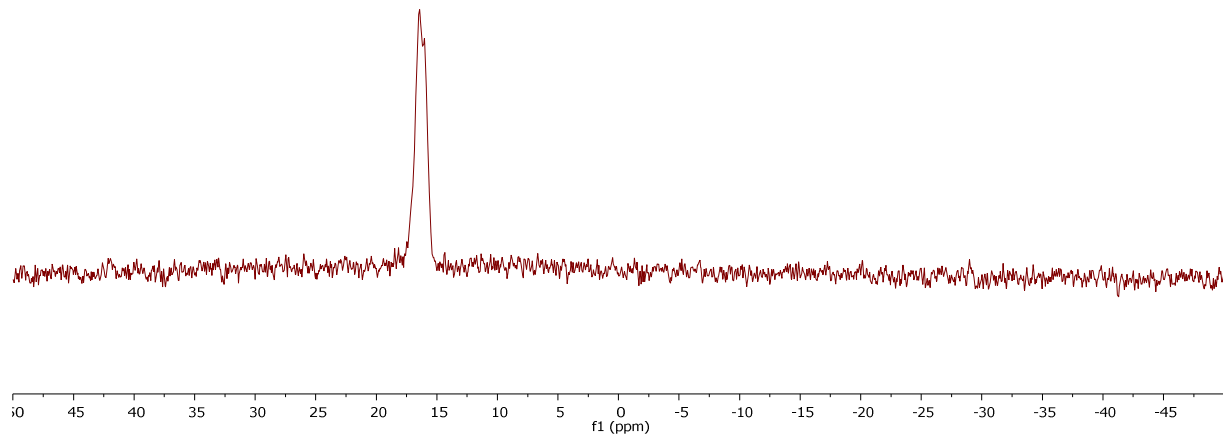


Figure S28. $^{31}\text{P}\{\text{H}\}$ NMR spectrum of **4B** (CDCl_3).

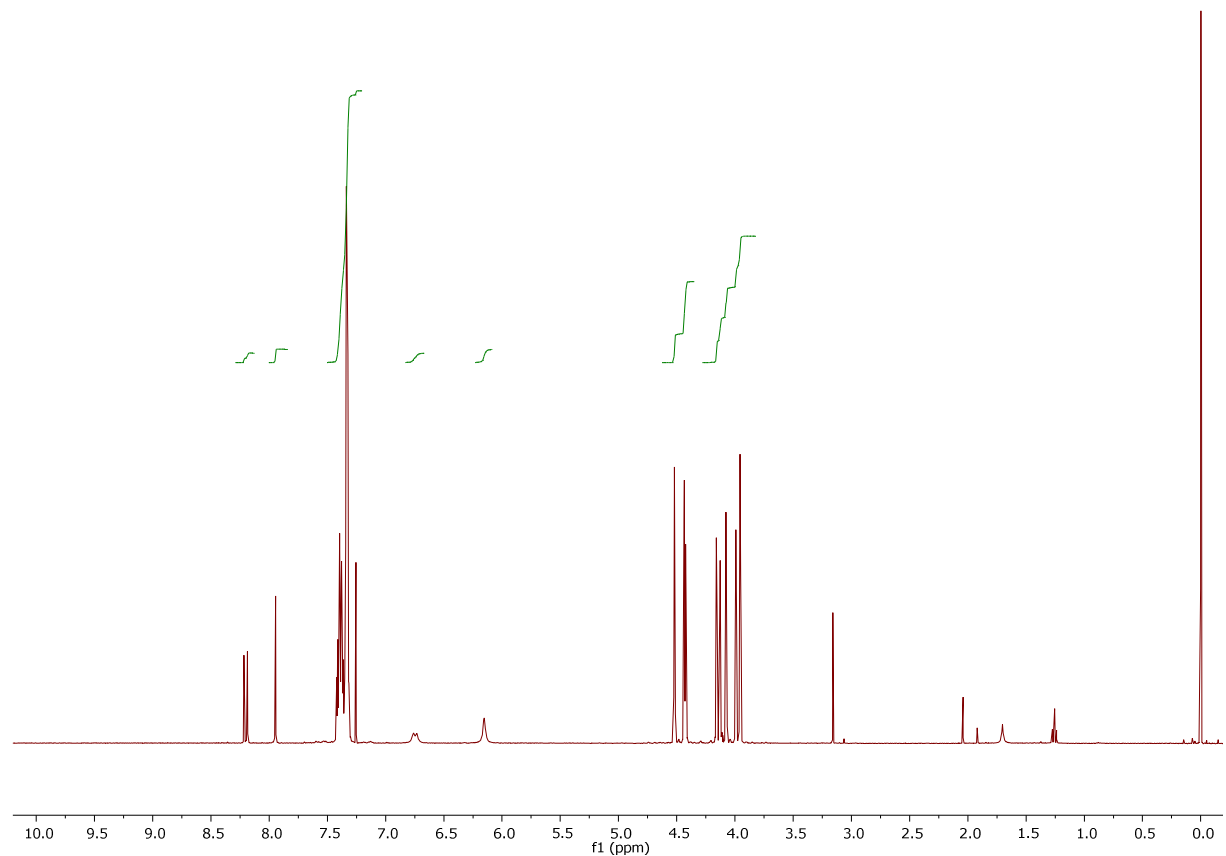


Figure S29. ^1H NMR spectrum of **5** (CDCl_3).

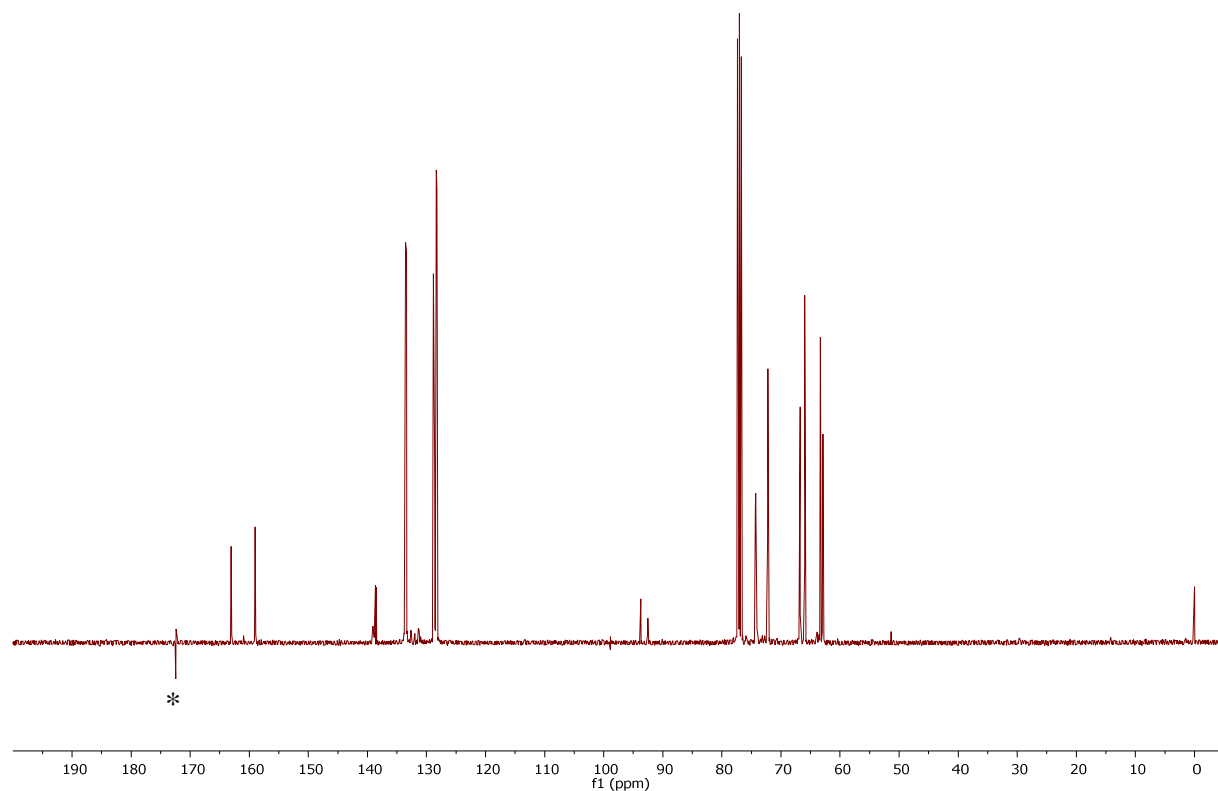


Figure S30. $^{13}\text{C}\{\text{H}\}$ NMR spectrum of **5** (CDCl_3 ; * = system peak).

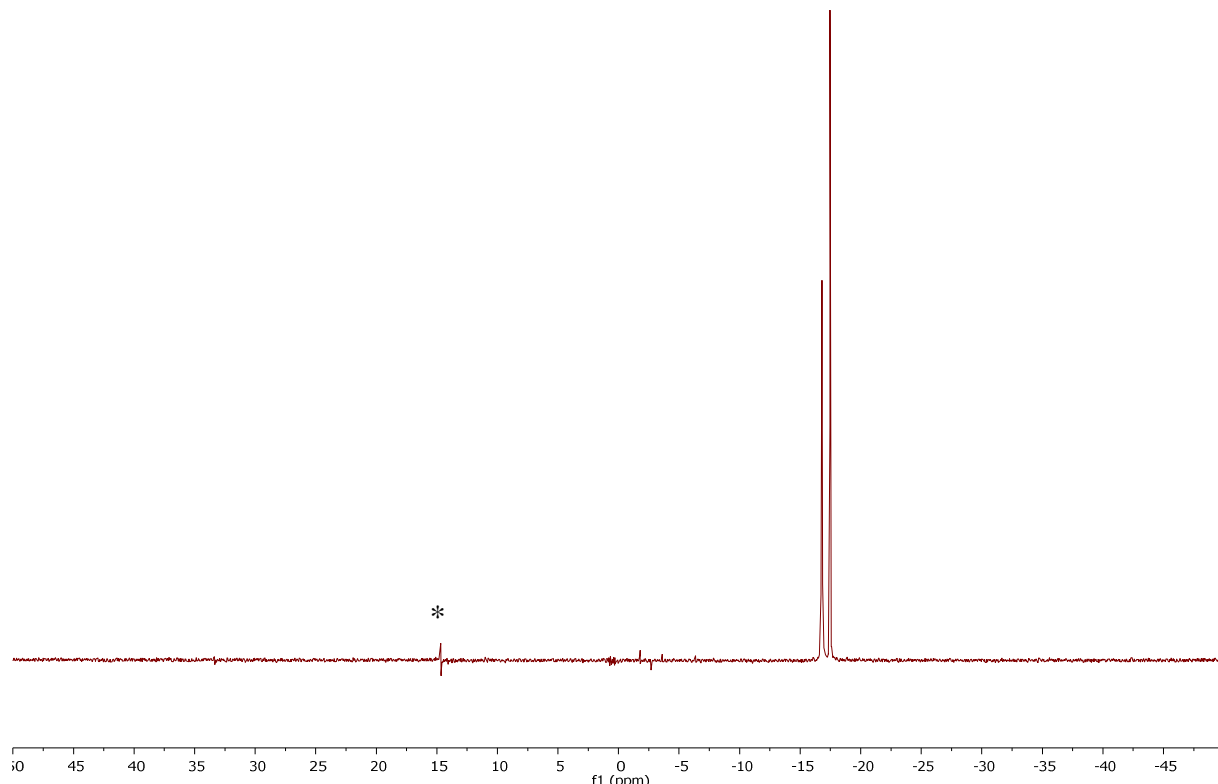


Figure S31. $^{31}\text{P}\{\text{H}\}$ NMR spectrum of **5** (CDCl_3 ; * = system peak).

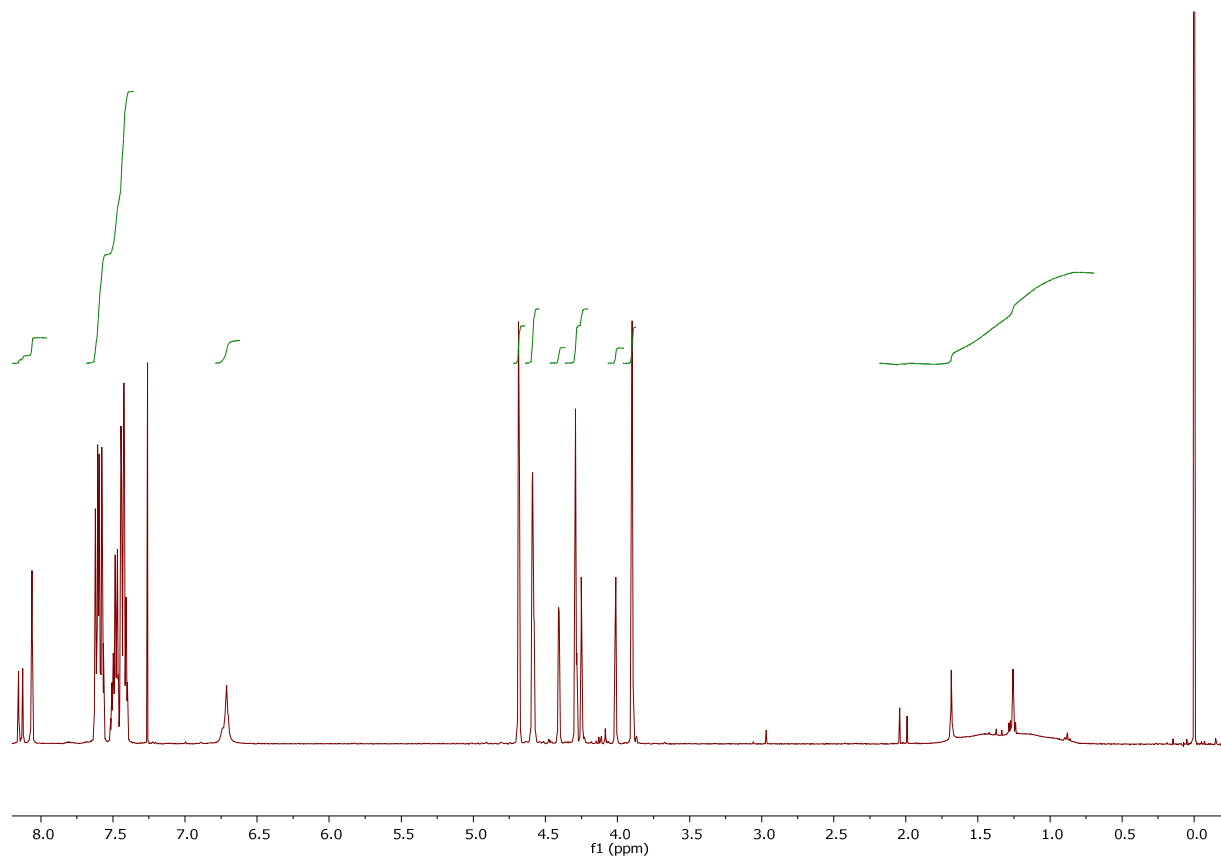


Figure S32. ^1H NMR spectrum of **5B** (CDCl_3).

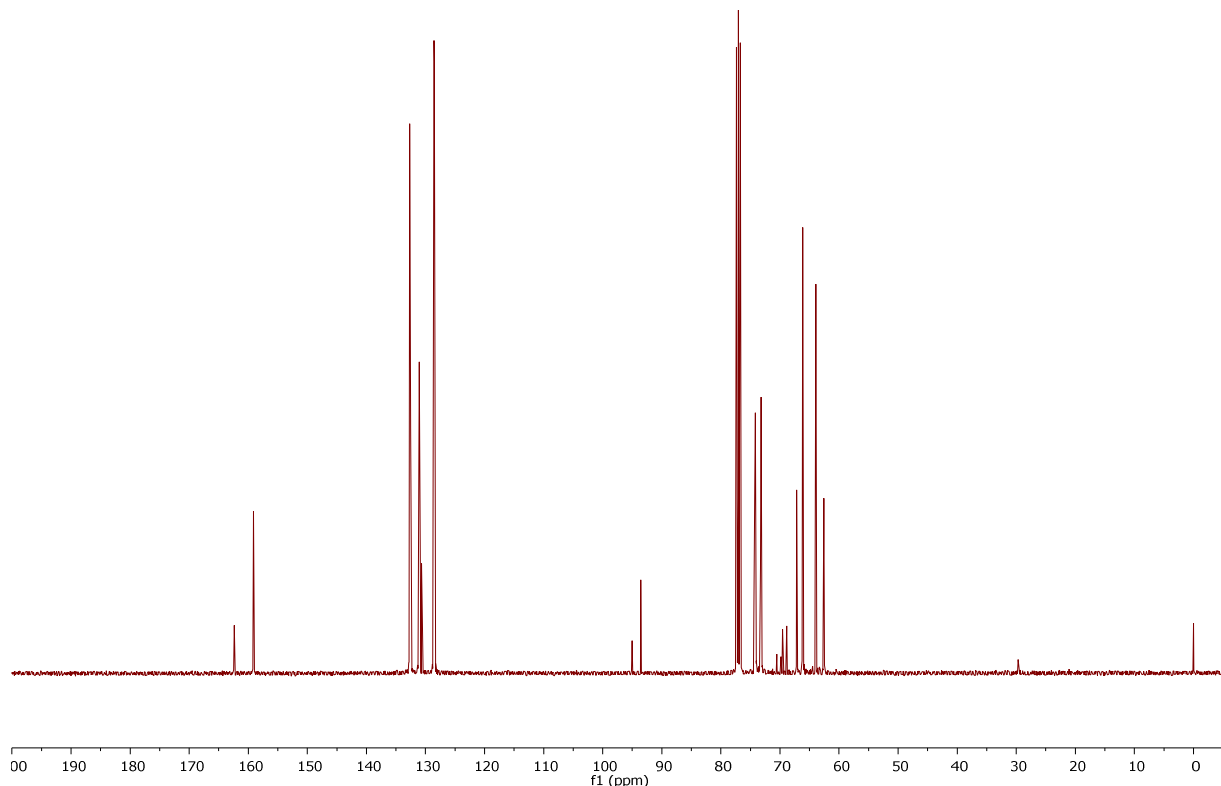


Figure S33. $^{13}\text{C}\{\text{H}\}$ NMR spectrum of **5B** (CDCl_3).

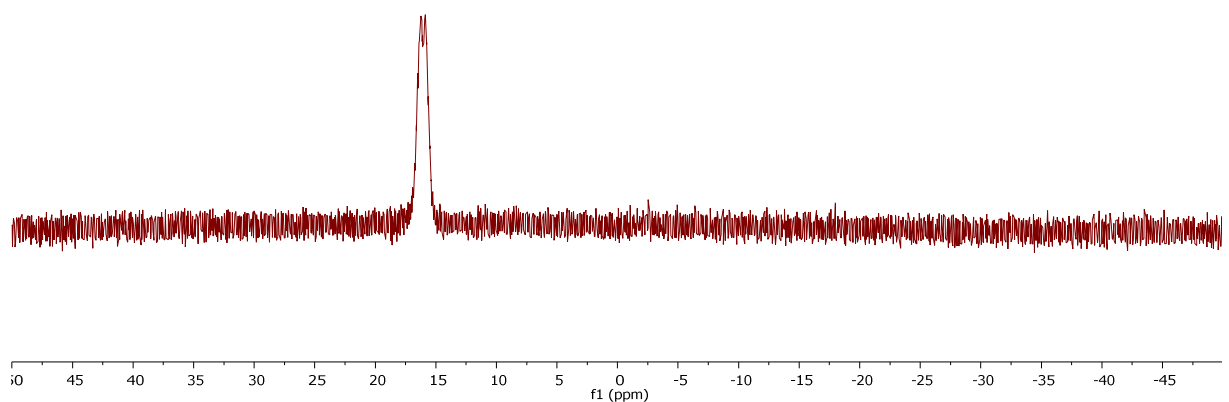


Figure S34. $^{31}\text{P}\{\text{H}\}$ NMR spectrum of **5B** (CDCl_3).

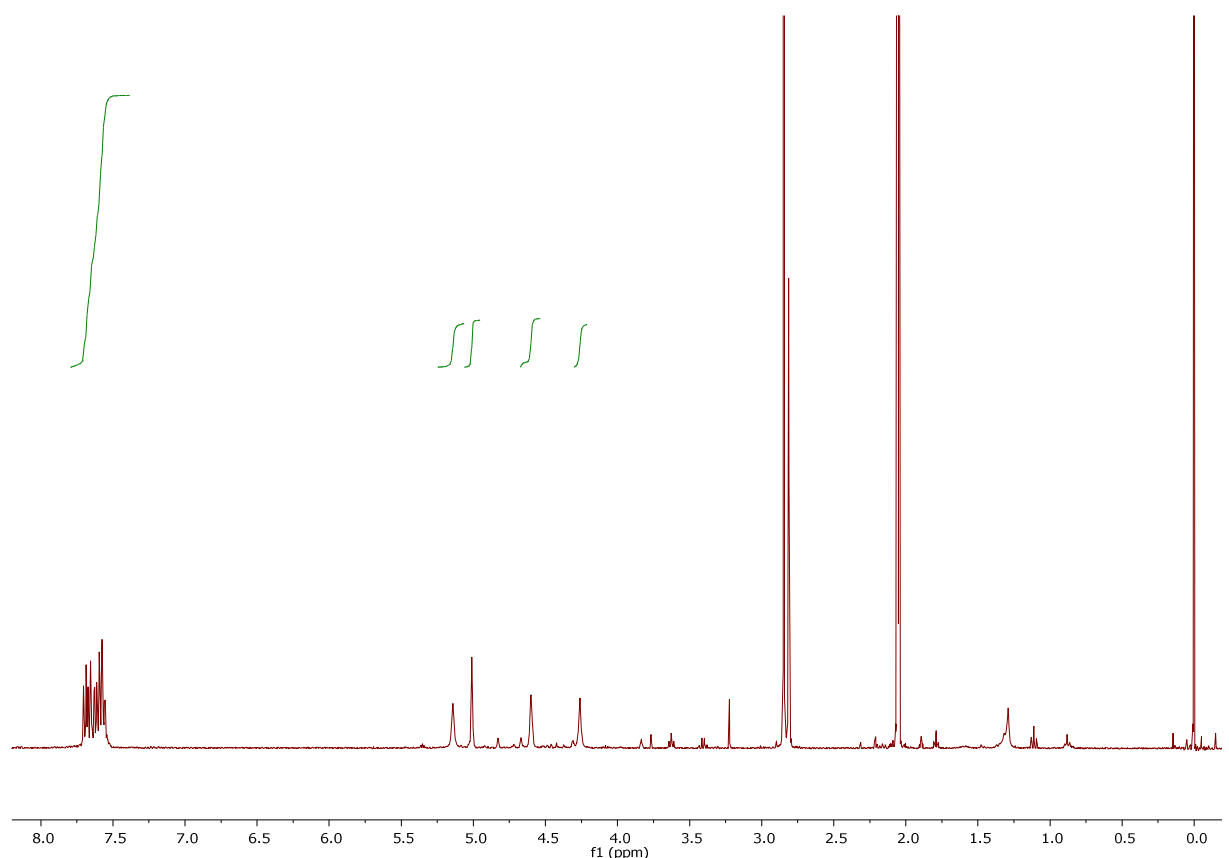


Figure S35. In situ ^1H NMR spectrum of **7** (acetone- d_6).

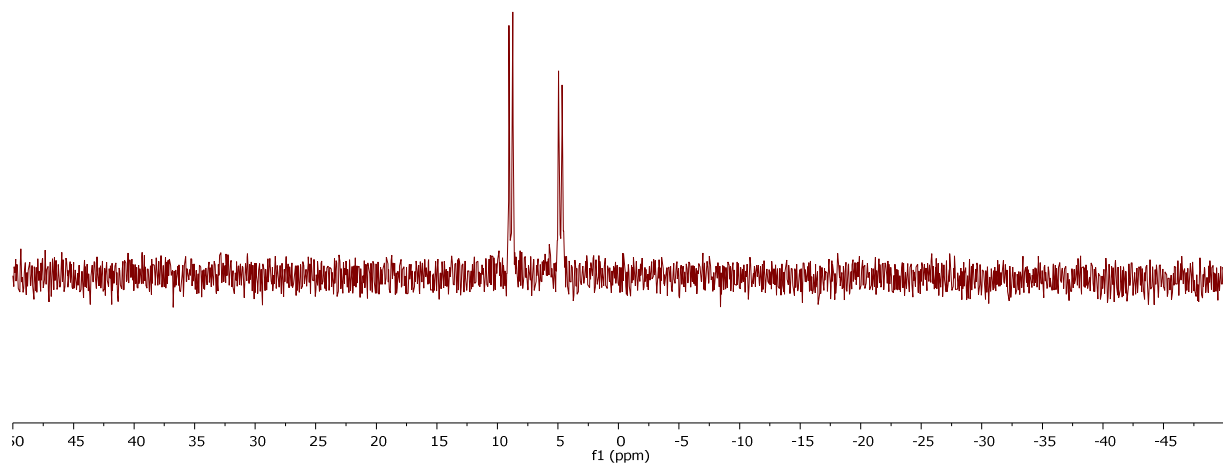


Figure S36. In situ $^{31}\text{P}\{\text{H}\}$ NMR spectrum of **7** (acetone- d_6).

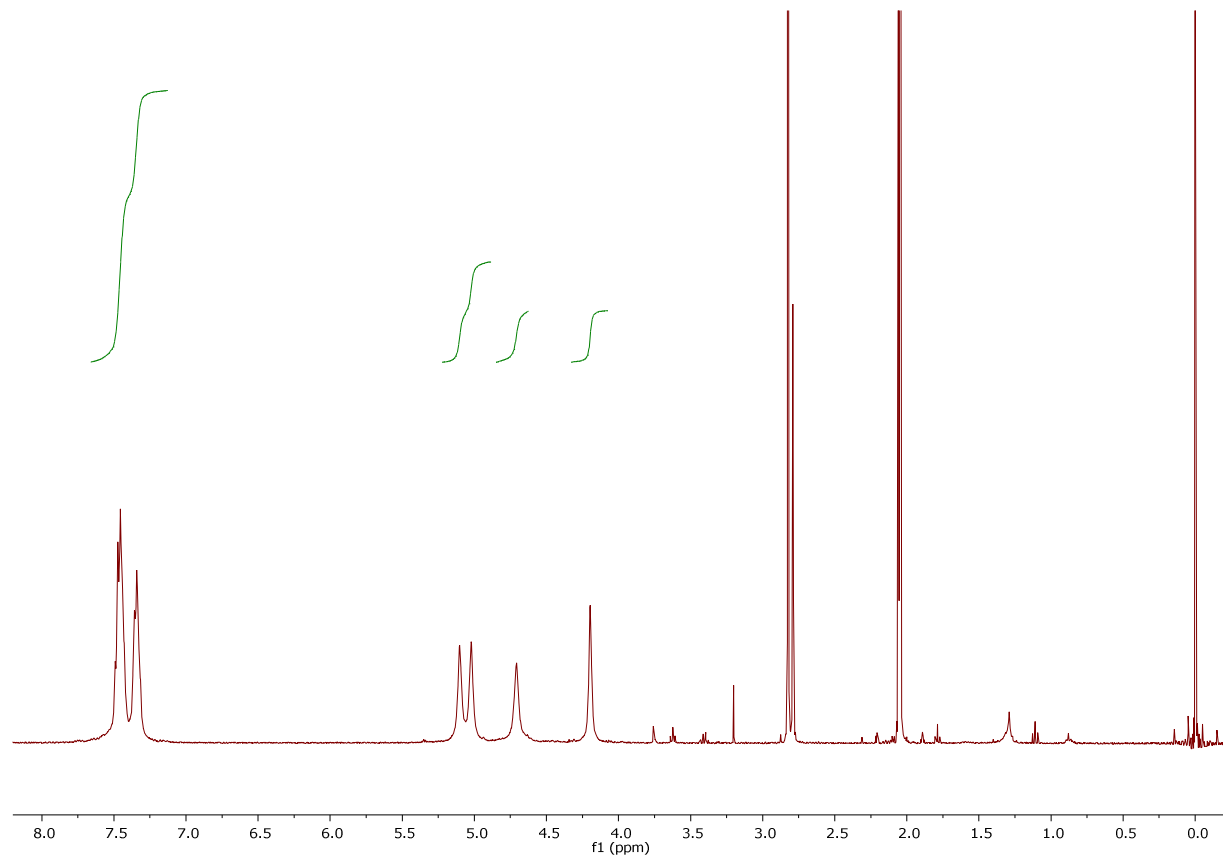


Figure S37. In situ ^1H NMR spectrum of **8** (acetone- d_6).

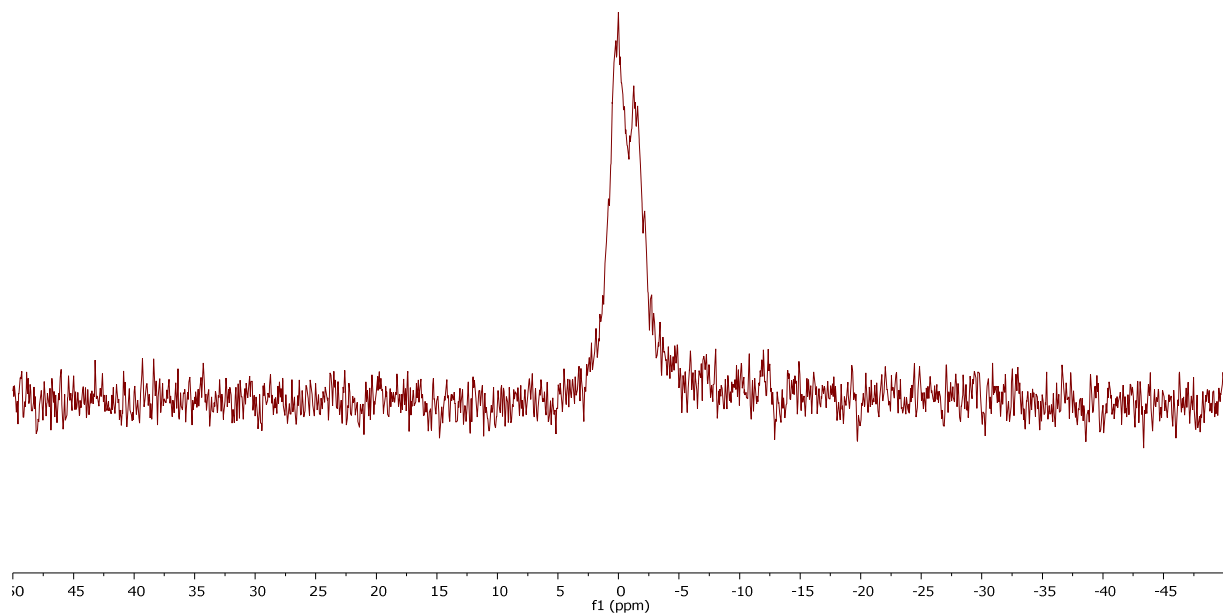


Figure S38. In situ $^{31}\text{P}\{\text{H}\}$ NMR spectrum of **8** (acetone- d_6).

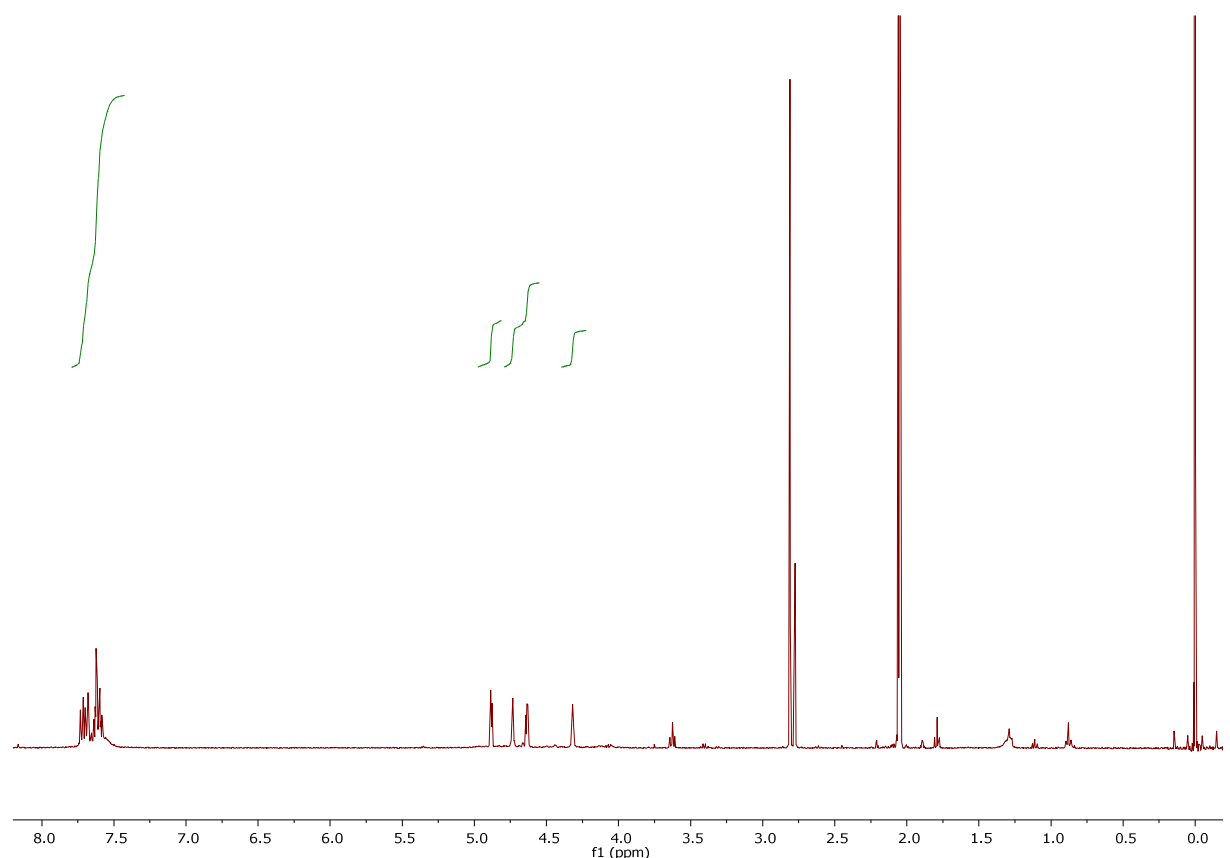


Figure S39. ^1H NMR spectrum of **9** (acetone- d_6).

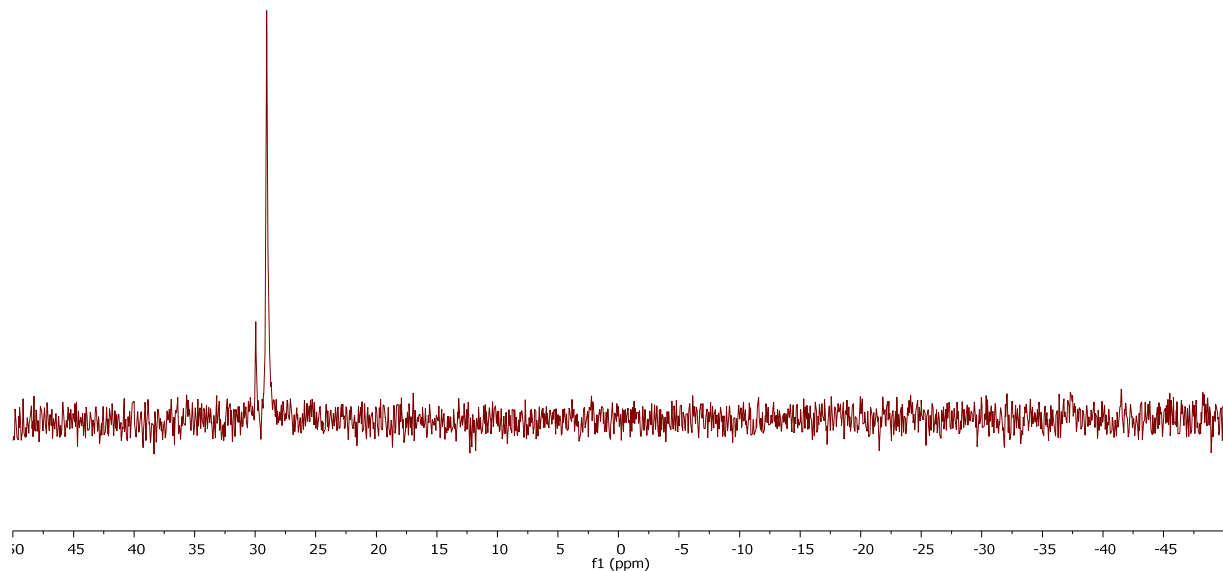


Figure S40. $^{31}\text{P}\{\text{H}\}$ NMR spectrum of (acetone- d_6).

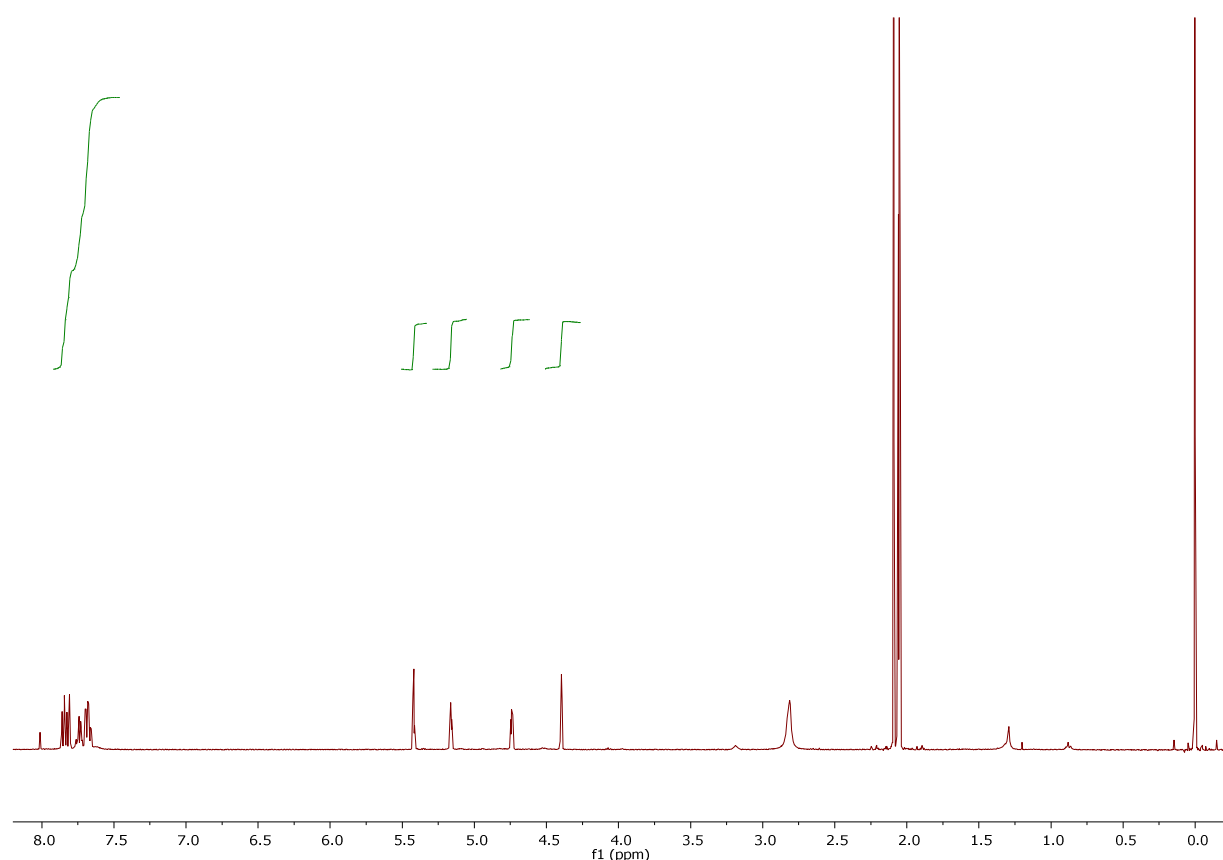


Figure S41. ^1H NMR spectrum of **11a** (acetone- d_6).

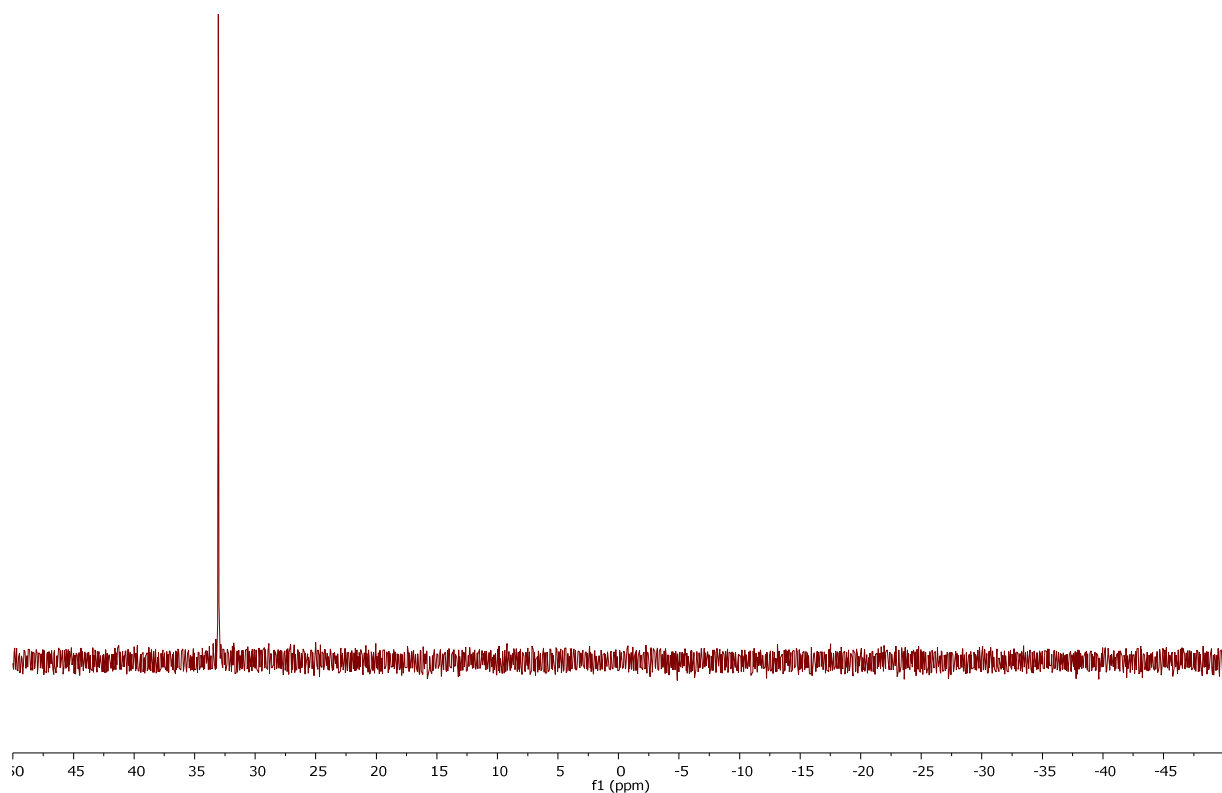


Figure S42. $^{31}\text{P}\{\text{H}\}$ NMR spectrum of **11a** (acetone- d_6).

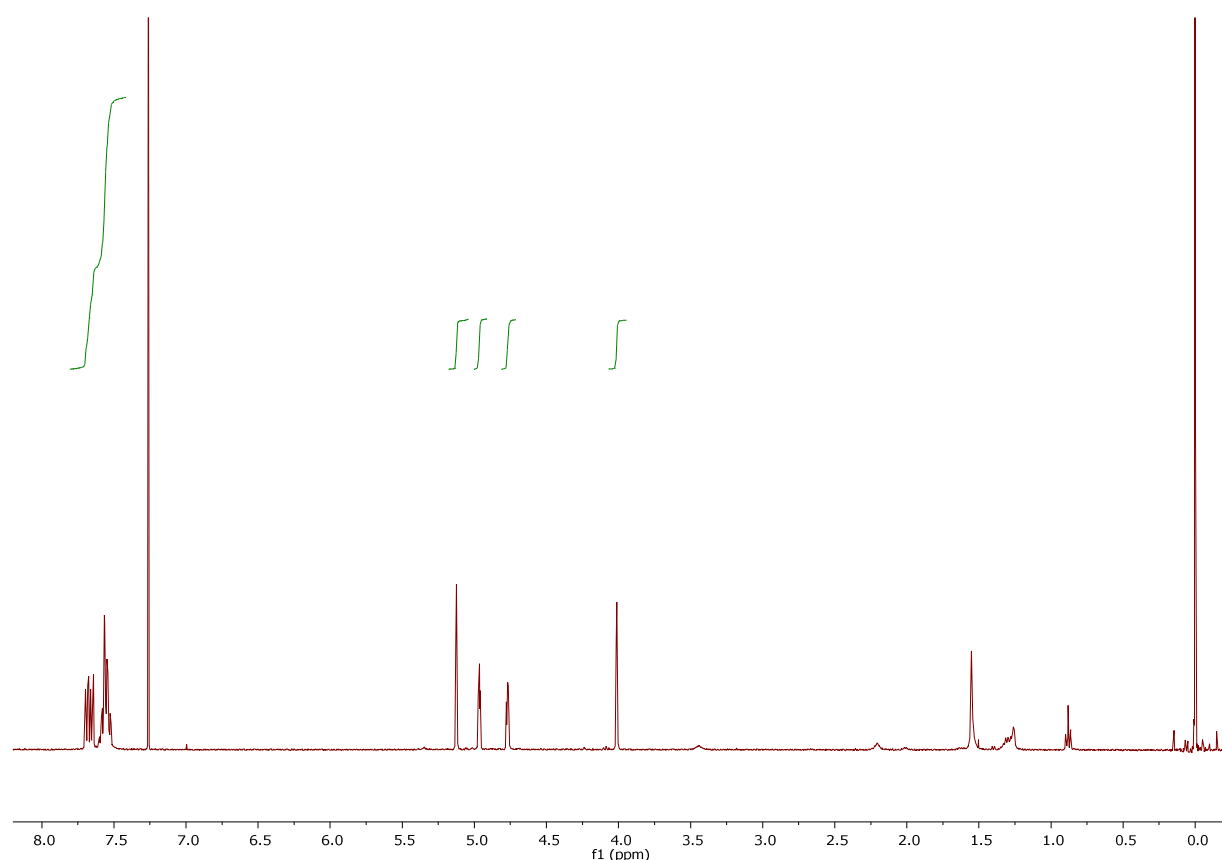


Figure S43. ^1H NMR spectrum of **11b** (CDCl_3).

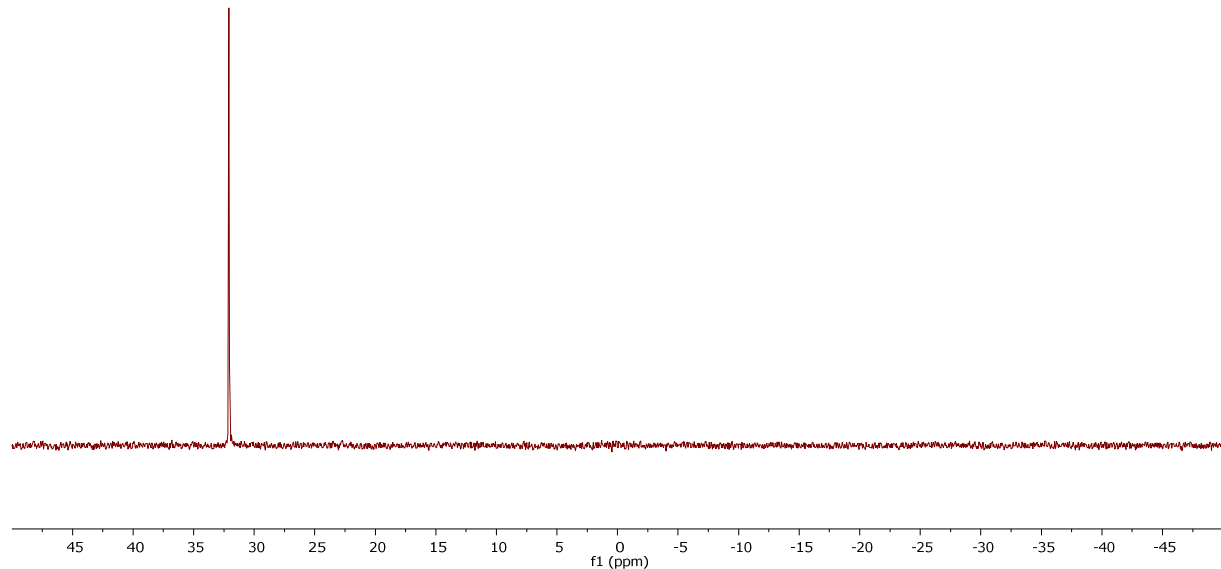


Figure S44. $^{31}\text{P}\{\text{H}\}$ NMR spectrum of **11b** (CDCl_3).

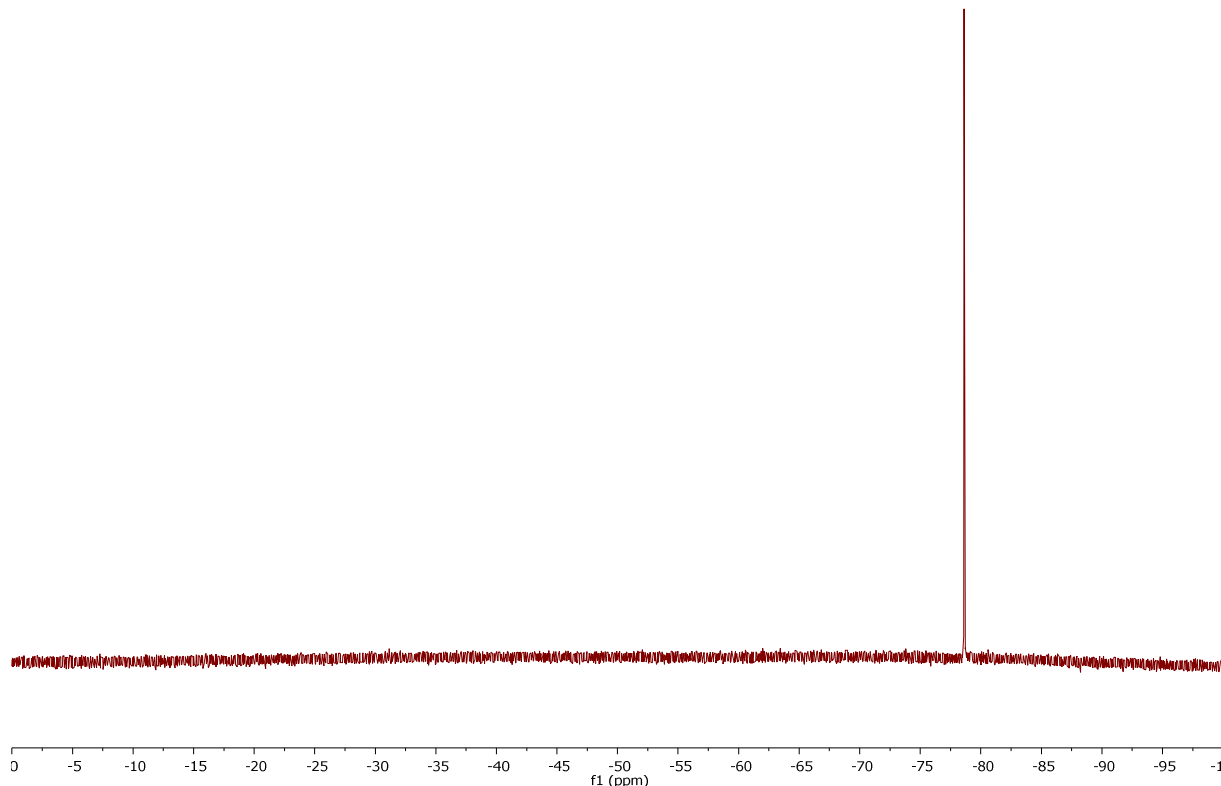


Figure S45. ^{19}F NMR spectrum of **11b** (CDCl_3).